

Chapter 10

From the climates of the past to the climates of the future

Sylvie Charbit, Nathaëlle Bouttes, Aurélien Quiquet, Laurent Bopp, Gilles Ramstein,
*Laboratoire des Sciences du Climat et de l'Environnement, LSCE/IPSL, CEA-CNRS-UVSQ,
Université Paris-Saclay, 91190 Gif-sur-Yvette, France.*

Jean-Louis Dufresne, *Laboratoire de Météorologie Dynamique / IPSL Université Pierre et
Marie Curie BP 99, 4 Place Jussieu 75252 Paris Cedex 05, France.*

Julien Cattiaux, *Centre National de Recherches Météorologiques, Université de Toulouse,
CNRS, Météo-France, 42 avenue Gaspard Coriolis 31057 Toulouse Cedex, France.*

This chapter connects everything we have learned about past climates (both from the analysis of natural archives and from numerical simulations), and future climate projections. The models used to explore the future are similar to those used for past climates, except that the results are based on emission scenarios of greenhouse gas emissions whereas past climate simulations may be compared to reconstructions from the natural archives described in volume 1. The climate of the past 1,000 years can be seen as the ‘background noise’ of the recent natural evolution of the climate system. On this basis, the current climate change can be analyzed. Over the longer term, analysis of ice cores allows us to trace back the history of atmospheric CO₂ concentration over the last 800,000 years, and shows that the anthropogenic disturbance (producing an atmospheric CO₂ concentration currently in excess of 410 ppm) is completely outside the documented glacial-interglacial variations over the last million years, ranging from 180 to 280 ppm. With this awareness you are well equipped to now explore the climate of the future.

10.1 Climate observations in recent decades: the first signs of warming

The principles of the physical laws governing the temperature on the Earth’s surface were formulated at the beginning of the 19th century by Joseph Fourier, who established that the energy balance at the surface of our planet is dominated by incoming solar radiation which is the primary source of energy, and infrared emission exchanges which control energy losses. He concluded that any change in surface conditions could lead to a change in climate and argued that *the development and progress of human societies can notably change the state of the ground surface over vast regions, as well as the distribution of waters and the great movements of the air and that such effects have the ability to cause the mean degree of heat to vary over the course of several*

centuries. Joseph Fourier also identified the trapping of infrared radiation by the gases in the atmosphere (Fourier, 1824).

This was the beginning of the greenhouse effect theory. Starting from this seminal work, numerous studies were conducted throughout the 19th and 20th centuries. Within a scientific context where the understanding of the glacial-interglacial cycles was the matter of a very hot debate, the Swedish chemist Svante Arrhenius was the first one to quantify the effect of the atmospheric carbon dioxide concentration on the average surface temperature of the Earth and to suggest that substantial variations of the atmospheric CO₂ levels could explain the glacial advances and retreats. However, it is only since the late 1970s that we can calculate precisely the radiation exchanges using radiative transfer codes and spectral databases to break down energy by wavelength.

Long time refuted, or at least underestimated, global warming has now become an incontrovertible reality: in 2001, the scientific review by the Intergovernmental Panel on Climate Change (IPCC) concluded that there was a growing body of evidence confirming global warming as well as other changes in the climate system. Based on the results of numerical experiments with coupled atmosphere-ocean general circulation models (AOGCMs), the Fifth IPCC Assessment Report, published in September 2013 (IPCC, 2013), established with a probability of more than 95%, that the global warming observed in recent decades is due to anthropogenic activities. This situation has no direct equivalent in the past climates of the Earth. The last time we find a climate with the current level of atmospheric CO₂ is several million years ago. The climate at this period corresponds to a warm Earth, with a reduced cryosphere (no Greenland) and a smaller Antarctic ice sheet yielding a much higher sea level (15 to 30 m higher as reported by Haywood *et al.* (2011, 2016).

10.1.1 Evolution of greenhouse gases

We have seen in previous chapters that the greenhouse effect is above all a natural phenomenon, without which the surface temperature of the Earth would be about -18°C, making life, as we know it today, impossible. The main greenhouse gases naturally present are water vapor (H₂O), carbon dioxide (CO₂) emitted by volcanic eruptions and forest fires, methane (CH₄) produced by wetlands and various fermentation processes, ozone (O₃), and the nitrous oxide (N₂O) emitted by soils. Industrialization has led societies to discharge massive amounts of these gases through the combustion of fossil fuels (oil, gas, coal), deforestation, agriculture, intensive livestock breeding and fertilizer production. An inhabitant of an industrialized country releases on average ten tons of carbon per year (or CO₂ equivalent) compared with only two tons per year for an inhabitant of most emerging countries. However, these estimates mask large disparities from one country to another, with differences ranging from 0.12 ton of CO₂ per year and per inhabitant for Ethiopia to 49.3 ton of CO₂ per year and per inhabitant for Qatar (from Global Carbon Atlas, 2017). In addition, human activities produce fluorinated gases (CFCs, HFCs, PFCs, SF₆) used especially in refrigeration and air conditioning systems, as well as in aerosol cans. In total, more than forty of these gases have been identified by the IPCC. The greenhouse effect produced by human activities is called *additional greenhouse effect*. The contribution of each gas to the additional greenhouse effect can be estimated by taking into account the increase in their concentration and their 'radiative efficiency'. Between 1750 and 2011, the variation in their concentration increased the greenhouse effect by about 2.83 W/m², with main contributions of

64% for CO₂, 17% for CH₄, 12% for O₃ and 6% for N₂O (Fig. 10.1). Since 1750, in other words, since the beginning of the industrial era, this anthropogenic phenomenon has produced an energy imbalance of the Earth and has caused a warming of the lower layers of the atmosphere. The additional radiative forcing corresponds to approximately 1% of the total radiation received.

Analysis of air bubbles trapped in the ice of the Antarctic ice sheet revealed that over the last 800,000 years, CO₂ levels have changed by no more than 100 ppm, going from 180 ppm during glacial periods to 280 ppm in interglacial periods. For periods prior to 1950, analysis of air bubbles in ice is the only reliable way to track the chemical composition of the atmosphere. In recent times, the first direct measurements (i.e. *in situ*) were obtained in 1958 at the Mauna Loa site in Hawaii (Keeling *et al.*, 1995). These measurements revealed for the first time that not only was CO₂ increasing in the atmosphere, but that this increase was modulated in line with seasonal variations due to photosynthesis of the terrestrial biosphere. This first measurement campaign was then supplemented by campaigns covering other sites in the northern and southern hemispheres. Currently, a wide range of direct and indirect measurements confirm that atmospheric CO₂ levels have increased since the beginning of the preindustrial era, rising from 275-285 ppm between the years 1000 and 1750, to about 380 ppm in 2005 (Fig. 10.1) and to more than 410 ppm in 2018, that is a difference of more than 100 ppm compared to the pre-industrial period. About 30 % of the current atmospheric CO₂ has been emitted by anthropogenic sources. In addition, the amount of annual anthropogenic emissions has been continuously increasing throughout the industrial era. In 1990, 2000, 2010 and 2017, global CO₂ emissions from human activities (fossil fuel combustion, cement production, land-use change) reached 22, 25, 32 and 37 GtCO₂/yr respectively. The increase in annual CO₂ emissions accelerated from 1.1 % per year in the 1990s to 3.3 % per year in the 2000s. This growth rate of atmospheric CO₂ is ten times faster than the highest rates recorded in ice cores, and is mainly due to the rapid growth of developing countries and a drop in the efficiency of fossil fuel use in the global economy. Between 65 % and 80 % of CO₂ released in the atmosphere is trapped and/or dissolved in the ocean and the terrestrial biosphere in 20 to 200 years, depending on the various estimations. The rest is removed by slower processes, including chemical weathering and rock formation that take several thousands of years, indicating that the effect of anthropogenic CO₂ will persist for hundreds to thousands of years into the future (Archer *et al.*, 2009).

Atmospheric methane is the third most important greenhouse gas after H₂O and CO₂ in terms of atmospheric concentration. Averaged over 100 years, the radiative efficiency of methane is estimated to be 28-36 times greater than that of CO₂ but its lifetime in the atmosphere (i.e. the time it takes for a CH₄ molecule to be removed from the atmosphere by chemical reaction) is much less (~9-12 years) than that of CO₂. Ice core records indicate that CH₄ levels in the atmosphere also show variations from about 350 ppb (during glacial periods) to 700 ppb (during interglacial periods). In 2011, the level of methane in the atmosphere, established from a network of measurements covering both hemispheres, was at 1,803 ppb, a level never attained, at least throughout the last 800,000 years. Since the pre-industrial era, CH₄ has increased by approximately 250%. Although the growth rate of methane was over 1% per year during the 1970s and early 1980s, the 1990s and early 2000s saw this rate stabilize, resulting in relatively stable concentrations. However, atmospheric CH₄ concentrations started growing again from 2007, although the true cause of this renewed increase is still unclear. CH₄ is emitted by many agricultural activities (ruminant farming, rice cultivation), by industrial activities (biomass combustion, the oil and gas industry), as well as by natural processes (wetlands, permafrost, peat

bogs). There are no available data on annual CH₄ emissions from industrial activities as these are difficult to quantify. When the climate heats up, CH₄ emissions from natural processes can increase. This has been observed with permafrost thawing in Sweden, but no large-scale evidence is available to clearly relate this process to the recent increase in methane. If the observed increase is caused by the response of natural reservoirs to global warming, this could last for several decades, even centuries, and thus reinforce the enhanced greenhouse effect (positive feedback).

The greenhouse gas with the fourth contribution to radiative forcing is nitrous oxide (N₂O). Its level has steadily increased from 270 ppb in 1750 to 323 ppb in 2011. The main natural emissions of this gas come from soil microbial activity and ocean processes. As for anthropogenic emissions, they come mainly from the use of nitrogen fertilizers in agriculture, fossil fuel combustion and chemical industry.

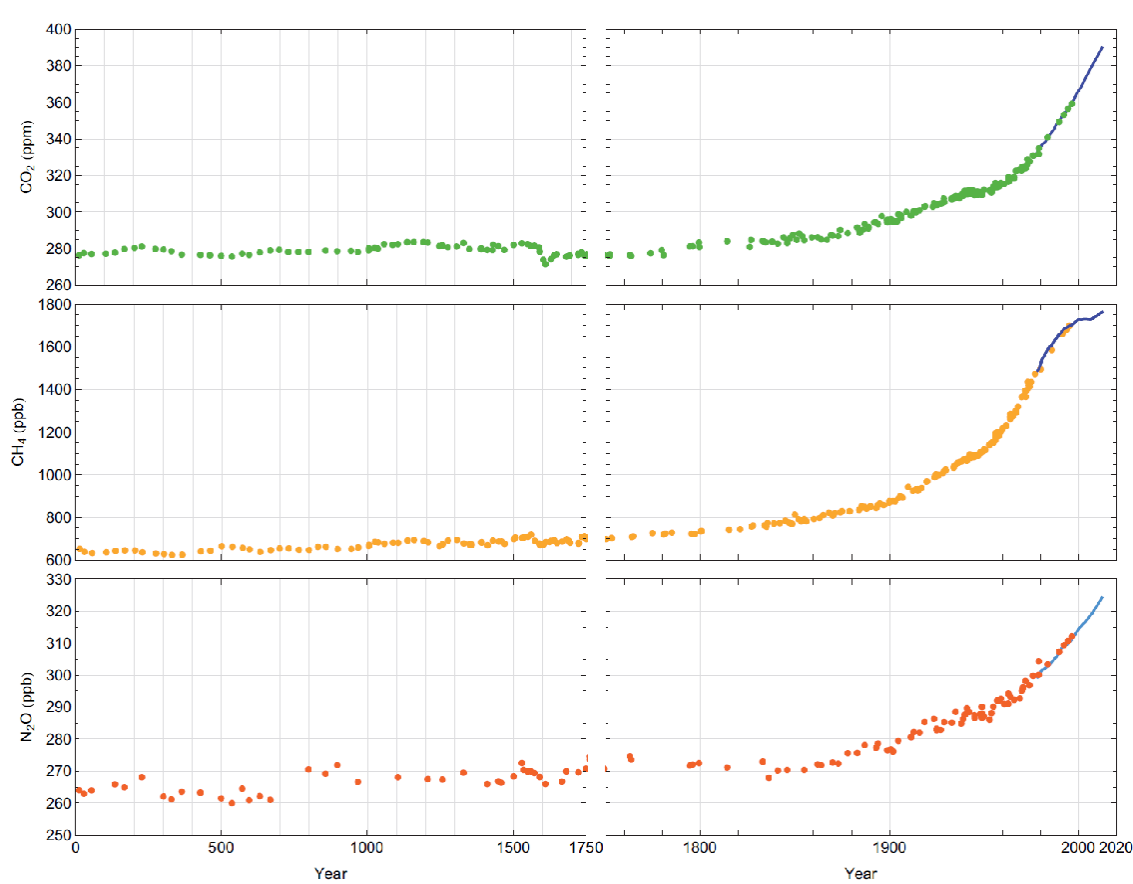


Fig. 10.1: Atmospheric CO₂ (*top*), CH₄ (*middle*), and N₂O (*bottom*) concentrations history since the beginning of the industrial era (right) and from years 0 to 1750 (left), determined from air trapped in ice cores and firn air (color symbols) and from direct atmospheric measurements (blue lines, measurements from the Cape Grim observatory) (Source: IPCC, 2013).

Halocarbons (or halogenated hydrocarbons), responsible in particular for the destruction of stratospheric ozone, generate a lower radiative forcing (about 0.35 W/m² in 2011) than the three main greenhouse gases (CO₂, CH₄ and N₂O), whose total contribution is 2.30 W/m². The emissions of these gases are almost exclusively anthropogenic. To combat the destruction of stratospheric ozone, the Montreal Protocol regulated the production of halocarbons containing chlorine

(chlorofluorocarbons or CFCs) and bromine. Substitute products adopted to replace CFCs, for example in refrigeration processes, do not affect the ozone layer but remain powerful greenhouse gases. Perfluorinated hydrocarbons (PFCs, such as CF_4 and C_2F_6) and sulfur hexafluoride have extremely long residence times in the atmosphere and are excellent absorbers of infrared radiation. Thus, even though these compounds are released in small quantities, their impact on the greenhouse effect and the climate is far from negligible.

Although ozone is also a greenhouse gas, it is not emitted directly, but is formed from photochemical reactions involving other precursor gases of natural and anthropogenic origin. Its impact on the radiative budget depends on the altitude at which the changes in its concentration occur, as these vary spatially. Moreover, once formed, its residence time in the atmosphere is very short, unlike the greenhouse gases mentioned previously. For this reason, it is difficult to establish precisely its role in the radiative budget.

In addition to the production of greenhouse gases, human activities also produce aerosols. These can have a direct impact on radiative forcing by absorbing or reflecting solar and infrared radiation. Some of them contribute negatively to radiative forcing, others positively. Finally, aerosols can have an indirect effect by modifying the reflective properties of clouds. Taking the totality of aerosols into account, the overall contribution is negative and therefore partially compensates the effect of greenhouse gases. In 2011, the estimated forcing of anthropogenic aerosols is about -0.9 W/m^2 , albeit with large uncertainties (-1.9 to -0.1 W/m^2 , IPCC, 2013). Overall, taking into account both greenhouse gases and aerosols, anthropogenic activities are responsible for a positive radiative forcing since the beginning of the industrial era, estimated at 2.3 W/m^2 in 2011 (IPCC, 2013). The main components involved in climate change are summarized in Figure 10.2.

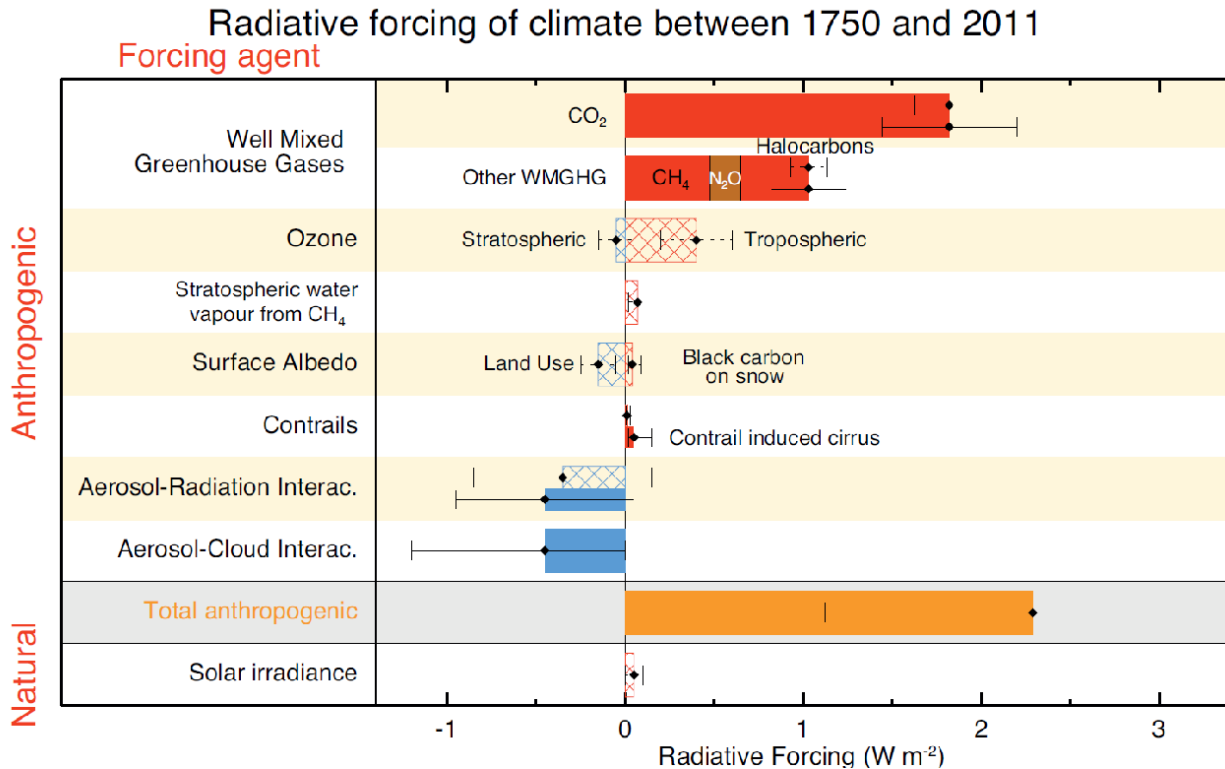


Fig. 10.2: Main components of radiative forcing involved in climate change coming from both natural processes and human activities. The values correspond to the estimated difference between 2011 and 1750. Anthropogenic contributions are responsible for most of the radiative forcing. Positive forcings cause global warming, while negative forcings lead to cooling. The black lines associated with each box show the associated uncertainties (Source: IPCC, 2013).

10.1.2 Evolution of surface temperatures

Instrumental observations documented for the past 150 years show an overall increase in temperature on the Earth's surface (Fig. 10.3). According to the synthesis presented in the Fifth IPCC Assessment Report (IPCC, 2013), it has increased by an average of $0.89 \pm 0.20^\circ\text{C}$ over the last century (1901-2012), that is an increase of about $0.08 \pm 0.02^\circ\text{C}$ per decade. This multi-decadal signal (warming trend) emerges as significant from the noise of the internal climate variability - a global warming is thus detected. Furthermore, dedicated studies have shown that the observed warming cannot be explained solely by natural forcings (solar and volcanic activities), and that anthropogenic forcings necessarily contribute: global warming is thus *attributed* to both natural and anthropogenic causes. In particular, “it is extremely likely that human activities caused more than half of the observed increase in global average surface temperature from 1951 to 2010” (IPCC, 2013). However, this increase has not been steady over time, due to decadal fluctuations in both the internal climate variability and the external natural and anthropogenic forcings. Indeed, the observations highlight two periods of accelerated warming: one from 1910 to about 1940, and the other, even more important, since 1970, while temperatures were relatively stable between 1940 and 1970 (Figure 10.3). Trends computed over short time periods are highly uncertain. For instance, the warming rate over the 15-year period 1998-2012 is about 0.05°C per decade, which is weaker than the 1901-2012 warming trend mentioned above (0.08°C per decade). However, the

associated confidence interval is large ($\pm 0.10^\circ\text{C}$ per decade), so that there is no inconsistency between both values. More generally, global warming is a long-term process that is superimposed on the internal climate variability, and it remains possible to have occasional short-term cooling trends in a warming world. Importantly, the decade of the 2000s appears to be the warmest compared to the entire period covered by instrumental data. The decade of the 2010s is likely to break this record, since the years 2014 to 2018 have been the five hottest years observed at global scale.

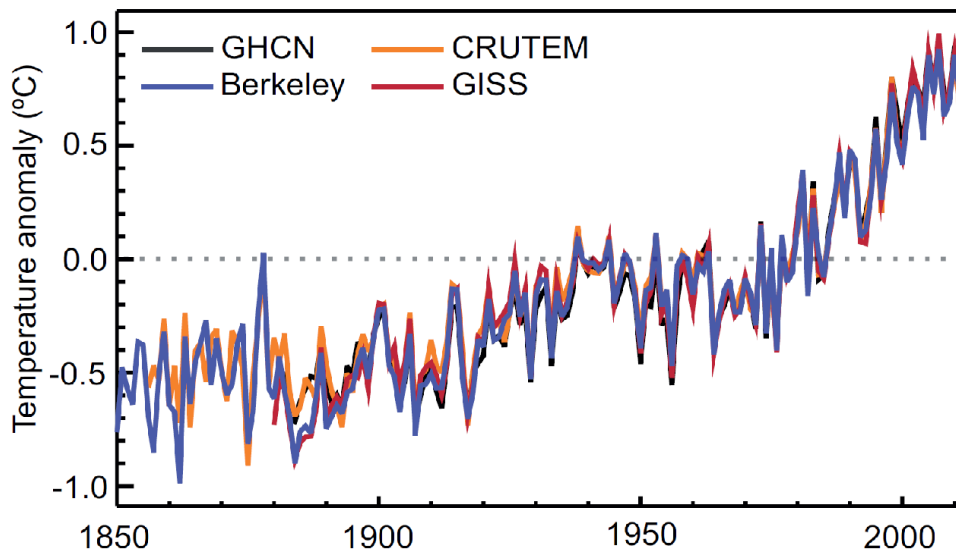


Fig. 10.3: Global annual average land-surface air temperature (LSAT) anomalies relative to the 1961–1990 climatology from the latest versions of four different data sets (Berkeley, CRUTEM, GHCN and GISS) (Source: IPCC, 2013).

The values mentioned above are global mean annual values. There are, in fact, large disparities from one region to another, as well as large seasonal disparities. In general, warming is amplified in high latitude regions in summer, partly due to the albedo effect induced by the decrease in snow cover and/or in the sea-ice extent. In addition, warming over the continents is much faster than over the oceans because of their weaker thermal inertia but also due to changes in evaporation. Not all regions exhibit a statistically significant warming over the observational period (e.g. South Greenland and North-West Atlantic); but no region exhibits a statistically significant cooling. Climate change detection is a signal-to-noise ratio problem: the higher the temperature variability, the harder it is to detect long-term warming. In other words, internal variability can hide climate change over small spatial domains and/or short time periods; but this does not call into doubt the existence of a long-term global warming trend, nor the fact that it is attributable to the anthropogenic fingerprint.

10.1.3 Evolution of temperature in the troposphere

In response to an enhanced greenhouse effect (e.g. due to anthropogenic activities), the physical theory of radiative transfer indicates that not only the surface, but the entire lower atmospheric layer, namely the *troposphere* (altitude 0-10 km), should warm. Conversely, the atmospheric layer above, namely the *stratosphere* (altitude 10-50 km), should cool. Observations

of the vertical temperature profile are more difficult to obtain than at the surface, but available data unanimously reveal a warming troposphere and a cooling stratosphere since the mid-20th century. This provides further evidence for the anthropogenic nature of the recent climate change. However, there has been a recent controversy about the amplitude of these changes. The IPCC's Fourth Assessment Report published in 2007 (IPCC, 2007) indicated persistent uncertainty on temperature trends in the middle atmosphere since 1979. Indeed, most of the available data from radiosondes and satellite measurements indicated a lower warming in the tropical high troposphere (between 10 and 15 km altitude) than that recorded at the surface, whereas all of the climate models projected an amplified warming in this zone of the atmosphere, especially in the tropics. This apparent difference between data and numerical outputs has been widely cited to emphasize the inconsistency between observational data and models. Some have used this example to call into question the impact of human activities on the climate, even going so far as to deny the existence of the current warming. But more in-depth analyzes have revealed that the observations on which this controversy was based were unreliable, particularly because the measurements did not take into account interannual climate variability. Since then, researchers have re-analyzed these measurements using more rigorous techniques (Allen and Sherwood, 2008). New estimates of these observations show greater warming than previously reported, and this new larger set of estimates now falls within the model trends, thus removing any concerns expressed in the 2007 Fourth IPCC Assessment Report.

10.1.4 Precipitations and water balance

While the increase in mean surface temperatures is one of the most obvious manifestations of ongoing climate change, spatial and temporal changes in the hydrological cycle (e.g. precipitation, evaporation, runoff) appear to be just as important but are much more difficult to simulate. The term precipitation refers to all the meteoric waters that fall to Earth in the form of liquid (rain, mist, showers) or solid (snow, hail, sleet) water. The formation of precipitation requires the condensation of water vapor around what are called condensation nuclei, which allow the water molecules to aggregate together. This phenomenon is called coalescence. Condensation only occurs when the amount of water vapor per unit of volume exceeds a threshold value, called the saturation value. This is an increasing function of temperature. Warmer air can therefore hold more water vapor before condensation occurs: this physical law is called the Clausius-Clapeyron relationship. For the Earth's atmosphere, the additional humidity that can be held by warmer air is estimated at 7 % per °C. Once the water vapor condensates, the different precipitation episodes can be categorized according to their intensity, duration, frequency, and by type (stratiform, like those caused by depressions in the mid-latitudes, or convective, like heavy rains and tropical cyclones in the intertropical convergence zone). These characteristics depend to a large extent on local temperature and weather conditions (wind speed and direction, pressure, humidity, evaporation). It is thus clear that a change in any of these parameters will affect the hydrological cycle as a whole.

Throughout the 20th century, for example, annual precipitation increased on the eastern side of the South and North American continents. In contrast, a significant rainfall deficit has been observed in south and west Africa, as well as in the Sahel. In northwestern India, an increase of about 20% was observed for the period 1901-2005, despite a sharp decrease between 1979 and

2005. However, changes in precipitation are hard to measure using the existing records, and there is only medium confidence that observed trends are due to the anthropogenic influence.

Observed trends in relative humidity (i.e. air humidity / saturation humidity) suggest that these have remained constant through the tropospheric column down to the surface. However, if the amount of water vapor at saturation increases and the relative humidity remains constant, then this means that the absolute humidity (and thus the amount of water vapor) has increased in the atmosphere. Observations indicate that tropospheric water vapor has increased by about 3.5 % over the past 40 years, which is consistent with the observed temperature change of 0.5°C over the same time period. Climate models confirm these empirical observations: a warmer climate leads to increased moisture content in the atmosphere and more intense precipitation events (although total precipitation over a full year is reduced) and therefore flooding is more likely to occur. Thus, in winter, it is observed that for most of the extratropical land surface areas of the northern hemisphere, the greatest precipitation is linked to higher temperatures. Conversely, in areas with low rainfall, such as the Mediterranean basin, rising temperatures are associated with a higher risk of drought. This general intensification of the hydrological cycle can be summarized by: wet gets wetter, dry gets drier.

Added to these complex phenomena is the variability in atmospheric circulation. In section 10.2.3.2, the modes of atmospheric variability will be examined in greater detail. However, we already know that fluctuations in atmospheric circulation over the North Atlantic brought heavy rainfall in the 1990s to northern Europe, and, in contrast, led to a drying-up of the Mediterranean basin. In addition, the severe Sahelian drought over more than 20 years (1970-1990) was linked to changes in both atmospheric circulation and surface ocean temperatures in all three of the Pacific, Indian and Atlantic basins. Although this trend towards drought still persists, it has become less pronounced since the early 1990s.

There are numerous uncertainties surrounding the determination of the hydrological cycle variables. This is due to a lack of data for some regions (for example, Canada, Greenland and Antarctica, some desert regions such as the Sahara, the Tibetan plateau and over the oceans), and to the fact that accurate measurements have only been available for a very short time. In addition, it is very difficult to measure precipitation rates and to accurately quantify their changes at the global and regional scales.

In situ measurements are affected by atmospheric conditions (e.g. the effect of strong winds especially on snowfall). Spatial observations, on the other hand, provide only instantaneous measurements and are affected by the uncertainties associated with the algorithms used to convert radiometric measurements into precipitation rates. Because of these difficulties, climatologists explore the coherence between the whole set of complementary variables associated with the hydrological cycle. One way to represent precipitation changes over the past century or over decades is to calculate the Palmer Drought Severity Index. This index is a measure of drought, in other words, the accumulated surface soil moisture deficit compared to average local conditions. It is based on recent rainfall and atmospheric humidity (determined from temperatures). In general, analyses of the last century suggest a trend towards drying for much of Africa, southern Eurasia, Canada and Alaska. Other direct or indirect measurements (e.g. from river flow estimations or ocean salinity measurements) show that during the 20th century precipitation has generally increased on land surfaces between 30°N and 85°N, but significant reductions have been observed over the last thirty or forty years between 10°S and 30°N.

At present, the main challenge is to determine the interannual variations and trends in precipitation changes over the oceans. Global averages are often unrepresentative and mask large regional disparities. However, particularly pronounced droughts in the last 30 years, as well as heavy rainfall events in many regions clearly illustrate an intensification of the hydrological cycle.

10.1.5 Extreme weather events

Extreme weather events result from exceptional fluctuations of a climate variable, and are generally associated with significant impacts on society and the environment. As illustrated by the frequent exposure by the media of the most impressive events, the statistical evolution of climate extreme characteristics (frequency, amplitude) is of major concern for current climate change, especially in the development of adaptation strategies. The term ‘weather extreme’ covers a wide spectrum of events at spatio-temporal scales ranging from intense local precipitation lasting a few hours to exceptional hot years for the whole planet. In addition, because they are by definition rare, extreme events offer few case studies, and the detection of possible man-induced trends requires analysis over long periods of time and/or large spatial domains. The study of extreme events is thus often restricted by the availability of datasets of sufficient spatial and temporal resolution.

10.1.5.1 Temperature extremes

Extreme temperature events typically affect large areas (usually several thousand kilometers), and are often accompanied by extremes in other climate variables (e.g. drought during a hot summer, snowstorms during a cold winter). Their impacts on ecosystems and human activities are thus particularly important.

One of the most striking recent examples is the European heat wave in summer 2003 which, with a temperature 2.5°C higher than the seasonal mean, exceeded by three standard deviations the distribution of summer temperatures in Europe. It had dramatic socio-economic and environmental impacts: high mortality, loss of energy production, acute urban pollution, fires, accelerated melting of glaciers etc. The return period of this particular event was estimated at 250 years at the time it occurred (2003); it would have taken 4 times longer (1000 years) without human intervention (Stott *et al.*, 2004).

This illustrates an expected feature of climate change: hot extremes become more frequent in a warmer world, and conversely, cold extremes become less common, but remain still possible. For instance, in the U.S., the ratio of the record of high maximum daily temperatures to the record of low minimum temperatures – which should be 1 to 1 in a stationary climate – is currently about 2 to 1 and is likely to reach about 50 to 1 by the end of the 21st century (Meehl *et al.*, 2009).

At the global scale the geographical distribution of changes in the frequency and amplitude of temperature extremes is consistent with the distribution of average warming (IPCC, 2013). This finding is nonetheless nuanced by the fact that changes in temperature distributions are often more complex than a uniform shift towards warmer values: spreading, tightening, and/or asymmetry of values may also show up in the statistical distribution. For instance, in Europe and Central U.S., the variability of summer temperatures is expected to increase in a warmer climate, due to the increase in evapotranspiration which leads to drier soils (Douville *et al.*, 2016). This would result

in a widening of the temperature distribution, and further amplify the increase in the frequency of hot extremes in these regions.

10.1.5.2 Precipitation extremes, tropical cyclones and extra-tropical storms

Changes in the frequency and intensity of droughts and floods, in response to global warming, are also of major concern, as our industrialized societies become increasingly vulnerable to rainfall extremes. Although the study of droughts is similar to that of heat waves, since they both have impacts over large areas, the analysis of extremes of intense precipitation is more difficult because it requires data with finer spatio-temporal resolution.

As illustrated by the record floods in summer 2002 in Europe, intense precipitation events have been on the increase since 1950 in the mid-latitudes of the northern hemisphere. Even in the Mediterranean Basin, where rainfall is decreasing on average, the episodes of heavy rainfall are more intense. A recent example is given by the intense precipitation that occurred in South of France in autumn 2018. This upward trend is noticeable on a global scale, although the increases are more moderate than those observed for temperature. Changes in precipitation extremes are consistent with the Clausius-Clapeyron relationship: warmer air can hold more humidity, so there is more water to be mobilized by condensation when rainfall events occur.

Paradoxically, the extent of regions affected by drought is also increasing, illustrating the fact that climate change not only affects the mean of statistical distributions, but also its variability. Africa, southern Eurasia and North America are, according to the IPCC Fifth Assessment Report, the regions most affected by these droughts in recent times, as illustrated by the dry conditions persisting from 2014 to 2018 over the west of the United States (California). The increase in the frequency and/or intensity of both intense rainfall episodes and droughts is consistent with the overall intensification of the hydrological cycle in a warmer world (wet gets wetter, dry gets drier).

Lastly, climate change may also affect meteorological systems like tropical cyclones or extra-tropical storms. In a warmer world, the former are expected to occur less frequently in general, due to less frequent atmospheric conditions favorable to the cyclogenesis (reduced temperature difference between the surface and the high-troposphere). However, once triggered, future cyclones should get more energy from a warmer ocean: the intensity of the strongest tropical cyclones is therefore expected to increase. Unfortunately, so far, trends are difficult to detect from the past due to the lack of homogeneous data. For extratropical storms, forecasting is even more difficult: projections performed with climate models do not unanimously agree on their frequency and/or intensity. The only robust future signal seems to be a poleward shift of the storm tracks, but again, available observations are insufficient to capture any past trend.

10.1.6 Evolution of the cryosphere

The exact estimate of the influence of human activities on climate is still limited because it is critically dependent on our ability to distinguish the signal related to this additional radiative forcing from the natural variability of the climate. However, there is a growing number of tangible factors indicating that man has had a perceptible influence on the climate. In particular, the global warming observed over the past century has been accompanied by a rise in sea level (Clark, 2016), largely attributed to the thermal expansion of the oceans, but also to significant changes in the

cryospheric components of the climate system over the whole planet. The cryosphere represents all the water in solid form on Earth and contains more than 70% of the Earth's freshwater reservoir. It is an excellent indicator of climate change. It includes ice sheets, floating ice-shelves, mountain glaciers, snow and sea ice, but also the water in rivers and lakes that freezes in winter and spring, as well as the permafrost, that is to say the permanently frozen ground, covered by an 'active' soil layer which melts each summer and whose thickness is variable.

Each of these components interacts in various ways with the other components of the climate system over a wide range of time scales, from seasonal (snow, permafrost, rivers, lakes, sea ice) to a hundred thousand years for the glacial-interglacial cycles. While the cryosphere is particularly important in the polar regions, there are also many glaciers in the low and mid-latitude regions, which provide an overview of the relationship between climate change and changes in the cryosphere.

10.1.6.1 Snow cover

Estimating the extent of snow cover and the physical properties of snow is of paramount importance for both hydrological applications, such as modeling or predicting runoff due to snowmelt, and for the understanding of local or regional weather patterns. Typical snow parameters, derived from radar data, include the extent of snow cover, the water equivalent of the snow, and the state of the snow (wet or dry).

The extent of snow cover has a direct influence on the energy balance on the Earth's surface, but also on the soil water content. Fresh snow reflects between 80 and 90% of incident solar radiation. The warming trend decreases the snow cover, which in turn decreases the fraction of solar energy reflected back to space, and increases the absorption of incoming radiation, thereby increasing warming, which in turn accelerates the snow melting. This amplifying mechanism is known as the 'temperature-albedo' effect. Thus, the surface temperature is strongly dependent on the presence or absence of snow. Another important aspect of snow cover is the role it plays in thermal insulation. In winter, snow covered ground cools much less quickly than bare ground, hence the importance of snow depth for plant and animal life. Finally, melting snow in spring and summer requires a high latent heat of fusion, so that the snow cover represents a significant heat loss for the atmosphere during the melting season. As a result, seasonal snow produces thermal inertia within the climate system, as it involves significant energy exchanges, with little or no change in temperature.

In the northern hemisphere, snow cover varies seasonally with a maximum in winter and a minimum in summer, but with large inter-annual variations. Since the end of the 19th century, daily records of snowfall and snow depth have been kept by many countries. Nevertheless, these measurements were only fully developed after 1950, and in particular from 1966 onwards, with the arrival of satellites.

All of these data series reveal that snow cover has decreased in the spring and summer since the 1920s, with an even more striking decrease since the end of the 1970s. According to the fifth IPCC Assessment report, this decrease in March-April snow cover extent ranges from – 0.8 % per decade over the 1922-2012 period to – 2.2 % per decade between years 1979 and 2012. For the fall and winter seasons, the signal is less clear: some data sets suggest positive trends as a result of increased snowfall in a warming climate, while others suggest negative trends similar to what is

observed in spring and summer. Nevertheless, there is a consensus that the mean annual snow cover has decreased with a shift from February to January of the maximum extent, an earlier onset of melting (~ 5.3 days since winter 1972-1973) and thus a reduction of snow cover duration. This drop in snow cover is mainly observed in the northern hemisphere. In the southern hemisphere, very few data exist outside of Antarctica, and these are often of much lower quality than in the northern hemisphere.

10.1.6.2 Evolution of sea ice

Sea ice is frozen seawater. When freezing occurs, salt is expelled from the ice crystals, thus raising the density of the surface ocean waters. The formation of sea ice can therefore have a direct impact on the intensity of the thermohaline circulation. Sea ice is a highly reflective surface with a high albedo of about 0.8. Conversely, when sea ice melts, the ice-free ocean surface absorbs about 90% of the radiation due to large albedo changes, causing the ocean to warm up, followed by a further increase in surface temperature. This phenomenon is a positive feedback between temperature and albedo. Thus, sea ice regulates heat exchanges between the atmosphere and the polar ocean. It isolates the relatively 'warm' ocean waters from the much colder atmosphere, except when there are winter 'leads' occurring as a result of sea-ice break-up. These leads allow the exchange of heat and water vapor between the atmosphere and ocean which can affect local cloud cover and precipitation rate.

The extent (i.e. area of the sea covered by sea ice), and the thickness of sea ice are the two indicators of sea ice conditions. Typically, the average sea-ice extent ranges from 14 to $16 \times 10^6 \text{ km}^2$ at the end of winter (7 to $9 \times 10^6 \text{ km}^2$ at the end of summer) for the Arctic and from 17 to $20 \times 10^6 \text{ km}^2$ (3 to $4 \times 10^6 \text{ km}^2$ at the end of summer) for Antarctica. The first systematic monitoring of sea ice conditions began in 1972 with the first satellite observations. For older periods, only a few scattered data are available. Most of the analysis of the variability and trends in sea ice cover relates to the post-1978 period. The results from different types of satellites give very consistent results, and all highlight an asymmetry between the Arctic and the Austral Ocean, with a clear decreasing trend for the Arctic and a slight growth for Antarctica, although the latter trend is not statistically significant.

Before the satellite era, sea-ice data are relatively sparse and inconsistent. Nevertheless, although these data indicate significant regional variability, all confirm an increase in sea-ice cover during the 19th century and the first half of the 20th century, and a sharp decline in sea ice from 1970 onwards. According to the assessment by the National Snow and Ice Data Center, sea ice coverage in September has decreased at a rate of ~ 12.8 % per decade from 1979 to 2018 relative to the 1981-2010 average (Fig. 10.4). One striking result was the record reached in 2007 when the total area of sea ice fell to $4.1 \times 10^6 \text{ km}^2$ in mid-September. In 2012, this record was broken with a minimum sea ice coverage of $3.4 \times 10^6 \text{ km}^2$ (i.e. ~ 20 % below the previous record) making 2012 the lowest minimum since the beginning of satellite era. Although, since 2012, measurements have not reached new records, the recorded September minima for sea ice extent for the 2015-2018 period are all below $5.0 \times 10^6 \text{ km}^2$. The persistence of these minima shows that the decrease in Arctic sea ice is accelerating. In the context of global warming, this observation is of growing concern for scientists, especially since the phenomenon is amplified by the temperature-albedo feedback. Moreover, in the past, a year marked by a very small sea-ice extent was generally followed the year after by a return to normal conditions. Observations made in recent years suggest

that a progressive disappearance of the oldest ice could occur if the decrease in sea ice continues at the same rate as in the last two decades.

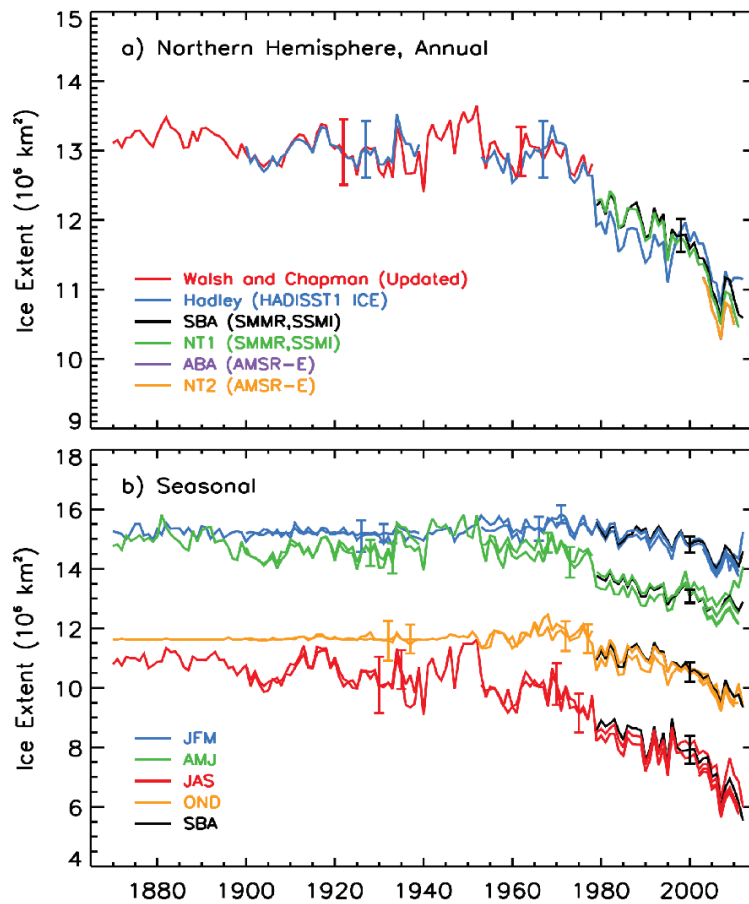


Fig. 10.4: Evolution of Arctic sea-ice extent from 1870 to 2011. (a) Annual sea-ice extent and (b) seasonal ice extent using averages of mid-month values derived from in situ measurements and remote sensing observations. In (b), data from the different seasons are shown in different colors to illustrate variation between seasons (blue : January-February-March; green: April-May-June; red: July-August-September; orange: October-November-December). The black lines in (a) and (b) correspond to data coming from the Scanning Multichannel Microwave Radiometer and passive microwave data from the Special Sensor Microwave Imager (Source: IPCC, 2013).

The decline in sea ice observed in recent years seems to be mainly driven by rising temperatures. However, atmospheric variability, and in particular the Arctic oscillation, may also favor the decreasing trend if the Arctic oscillation is in a positive mode. This has the effect of shifting the jet stream from the mid-latitudes to higher latitudes and causes the older, thicker sea ice to be pushed out of the Arctic. More recent, thinner ice remains in the region and is more prone to disappear during the melt season (Rigor and Wallace, 2004). Between 1989 and 1995 the Arctic Oscillation entered a very positive mode, thereby reducing the extent of sea ice. Since the mid-1990s, only a few years have seen a positive or a neutral mode. Meanwhile, the thickness of Arctic sea ice continues to drop due to increasing temperatures. In March 1985, the fraction of first-year

ice was ~50 % against 70 % or more in 2015, and during the 1985-2015 period, the multi-year ice (4 years and older) dropped dramatically from 20 % to only 3 % (Tschudi *et al.*, 2016).

The situation is different in Antarctica mainly because of its geographic location (surrounded by the Southern Ocean and centered on the South Pole). Atmospheric winds and the oceanic circumpolar currents act as barriers to warmer air and warmer waters coming from the north. Changes in sea-ice coverage are more tenuous, with an increase of 1.2 to 1.8 % per decade between 1979 and 2012 (IPCC, 2013). However, changes in the distribution of Antarctic sea ice show major regional differences. For example, the Weddell and Ross seas are experiencing an increase in sea ice extent due to large-scale changes in atmospheric circulation, while in West Antarctica, the surface covered by sea ice is drastically decreasing, consistent with the observed warming in this region.

10.1.6.3 Permafrost

Permafrost is defined as soil that remains permanently frozen for at least two consecutive years. It is topped by a so-called 'active layer' that thaws each summer, and whose thickness can vary from a few centimeters to a few meters, depending on altitude and latitude. In areas where it has persisted for several glacial-interglacial cycles, the permafrost can be several hundred meters thick, and even exceed 1000 m in some parts of Siberia and Canada. During the last glacial-interglacial cycle, there have been large variations in area and depth of permafrost over North America (Tarasov, 2007) or Europe (VandenBerghe, 2001). Currently, permafrost covers 22.8×10^6 km² of the northern hemisphere, or about 24% of the continental areas. Permafrost occurs mainly in polar and circumpolar areas and in mountain regions at lower latitudes (e.g. Chile, the Alps, the Himalayas). It can also be found in the seabed of the Arctic Ocean in the continental shelf areas. When surface conditions are not spatially homogeneous (e.g. snow cover, vegetation) permafrost can occur in patches. Such permafrost areas are called 'discontinuous permafrost zones'. When temperatures drop at higher latitudes, gaps in permafrost are less frequent. When surface conditions become homogeneous, permafrost is referred to as 'continuous permafrost'.

The presence of permafrost is critically dependent on the soil temperature, which is itself controlled by the surface energy balance, and thus, by several climatic factors such as incoming solar radiation, cloudiness, snow cover, vegetation cover, surface and subsurface hydrology, and carbon exchanges between the soil and the atmosphere. One of the key factors affecting permafrost distribution is the insulating effect of snow. When snow is present, ground temperatures are generally warmer than those which would occur under smaller snow cover or snow-free conditions. In continuous permafrost areas, snow cover exerts a direct influence on the active layer thickness. For example, it has been shown that a doubling of snow cover from 25 to 50 cm may increase the mean annual surface soil temperature by several degrees (Fig. 10.5). On the other hand, if seasonal snow melting occurs in late spring or early summer, ground warming is delayed.

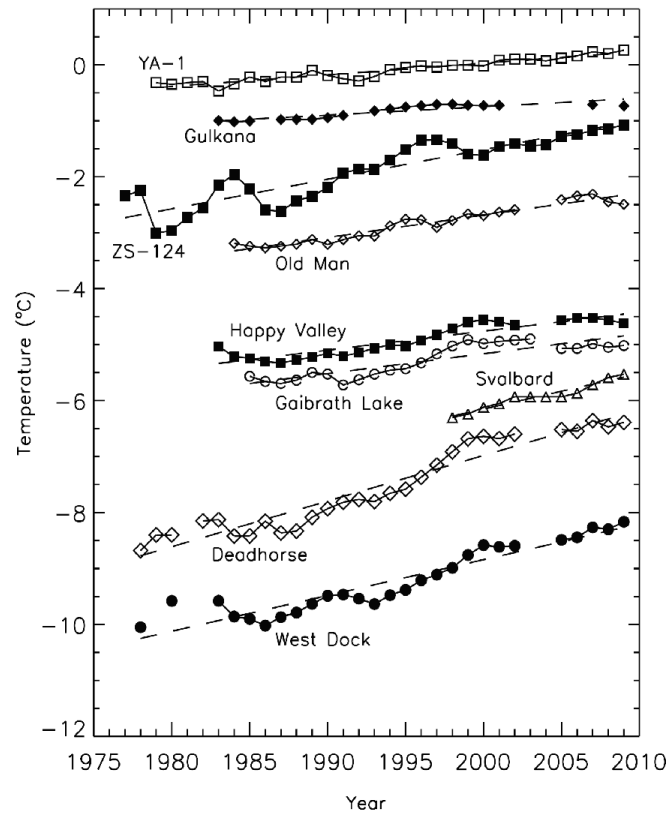


Fig. 10.5: Time series of mean annual ground temperatures at depths between 10 and 20 m for boreholes located throughout the circumpolar northern permafrost regions (Romanovsky *et al.*, 2010a). Data sources are from Romanovsky *et al.*, (2010b) and Christiansen *et al.*, (2010). Measurement depth is 10 m for Russian boreholes, 15 m for Gulkana and Oldman, and 20 m for all other boreholes. Borehole locations are: ZS-124, 67.48°N 063.48°E; 85-8A, 61.68°N 121.18°W; Gulkana, 62.28°N 145.58°W; YA-1, 67.58°N 648°E; Oldman, 66.48°N 150.68°W; Happy Valley, 69.18°N 148.88°W; Svalbard, 78.28°N 016.58°E; Deadhorse, 70.28°N 148.58°W and West Dock, 70.48°N 148.58°W. The rate of change (degrees Celsius per decade) in permafrost temperature over the period of each site record is: ZS-124: 0.53 ± 0.07 ; YA-1: 0.21 ± 0.02 ; West Dock: 0.64 ± 0.08 ; Deadhorse: 0.82 ± 0.07 ; Happy Valley: 0.34 ± 0.05 ; Gaibrath Lake: 0.35 ± 0.07 ; Gulkana: 0.15 ± 0.03 ; Old Man: 0.40 ± 0.04 and Svalbard: 0.63 ± 0.09 . The trends indicate the very likely range, 90% (Source: IPCC, 2013).

The permafrost thermal state is also influenced by rainfall. Firstly, ground temperatures can be increased through the energy flux released by liquid precipitation penetrating into the soil. Secondly, rain falling on a snow covered surface may alter the snow insulating effect causing temperatures to lower. Interception of precipitation by vegetation also has an impact on ground temperatures through evaporation and transpiration and the associated turbulent heat exchanges between atmosphere and surface layers. However, the direct effect of vegetation on ground temperatures is less important than its role on snow cover. Interception of snow in boreal forests reduces snow cover on soils and acts to reduce ground temperatures. These examples show that the formation or degradation of permafrost is strongly influenced by climate. It is thus studied as an indicator of climate change by a global network of researchers (Romanovsky *et al.*, 2010a, b) who rely on temperature measurements taken from boreholes and from satellite tracking. In the framework of the International Polar Year (2007-2009), a large permafrost- monitoring network

was developed and ground temperatures (which control the thermal state of the permafrost) have been measured in 575 sites located in arctic regions (North America, Nordic Eurasian regions and Russia). In most sites belonging to the network, permafrost temperatures have increased in recent decades. The observed rate of change of mean annual ground temperatures from mid-1970s to 2010 ranges from 0.15 ± 0.03 to 0.82 ± 0.07 °C per decade, depending on the site (Figure 10.5). In cold permafrost regions (mostly in continuous permafrost zones), the mean annual ground temperatures have increased by up to 2°C, compared to less than 1°C in warm, forested permafrost areas (discontinuous permafrost). This can be explained by the fact that the amount of ice in warm permafrost is usually larger than for cold permafrost. Indeed, in case of ice melting, the overall warming trend is counteracted by the latent heat effect. Moreover, in forested areas, the snow insulating effect is limited due to the interception of snow by vegetation.

One of the main consequences of permafrost warming is increased thickness of the active layer, although some permafrost areas exhibit only modest thickening or even a thinning. Indeed, a study based on the analysis of 169 circumpolar and mid-latitude sites revealed that only 43.2 % of them have experienced an increase of the active layer thickness since the 1990s (Luo *et al.*, 2016). However, there is great spatio-temporal variability from one site to the other ranging from a few tenths of cm/yr to more than 10 cm/yr. Thickening of the active layer is a matter of great concern since it may have large consequences on the stability of the surface due to the melting of shallow ground ice. Potential impacts include thaw settlement, soil creeps, slope failures and ponding of surface water. All these features can cause severe damages to infrastructures, such as roads, dams or structural building foundations but also to vegetation. In forested areas, thaw modifies the hydrological conditions and can lead, for example, to the destruction of tree roots, causing drastic changes in the ecosystems. When permafrost thaws and the active layer thickens, more organic matter is likely to be decomposed by bacteria that produce either methane or carbon. In both cases, the bacterial action enhances greenhouse gas emissions and thus promotes global warming. However, the magnitude of this thaw-related feedback is a great unknown. The total amount of carbon stored in the permafrost has been estimated at 1,672 Gt, of which 277 Gt is found in peat bogs. This is about twice the amount of carbon in the atmosphere.

We still do not know for sure if the increase in atmospheric methane concentration observed in recent years, after about ten years of relative stability, is due to the warming of the high northern latitudes. Another amplification reaction observed at high northern latitudes involves the microbial transformation of nitrogen trapped in soils into nitrous oxide, which could increase with increasing temperatures and thus, in turn, amplify global warming.

In any case, even if there are still many uncertainties, the fifth IPCC assessment report emphasized on the positive feedback of permafrost melting on climate warming: “*the release of CO₂ or CH₄ to the atmosphere from thawing permafrost carbon stocks over the 21st century is assessed to be in the range of 50 to 250 GtC for RCP8.5*” (IPCC, 2013).

10.1.6.4 Glaciers

A glacier is a mass of ice formed by the successive accumulation of layers of snow year after year. Over the years, under the pressure of its own weight, the snow hardens and becomes granular (firn), then turns into ice and expels the air it contained. Under the action of gravity, the ice flows along the slope, thus supplying the lower parts of the glacier. A glacier is in constant movement

and carries mass from high altitudes to lower altitudes. In winter, the glacier grows due to snow accumulation on its surface. During the following summer, the glacier loses all or part of the mass it gained during winter. The disappearance of ice through surface processes is called ablation. The difference between accumulation and ablation determines the surface mass balance of the glacier. This brings about a change in ice volume. A positive balance overall causes the glacier to grow while a negative balance leads to a loss of ice volume which can be accompanied by a retreat of the glacial front.

The mass balance of temperate glaciers in the mid-latitudes is mainly dependent on winter precipitation, summer temperature and summer snowfalls (temporally reducing the melt due to the increased albedo). In contrast, the glaciers in low latitudes, where ablation occurs throughout the year and multiple accumulation seasons exist, are strongly influenced by variations in the atmospheric moisture content which affects incoming solar radiation, atmospheric long-wave emission, albedo, precipitation and sublimation. In monsoon areas, such as the Himalayas, accumulation and ablation occur mainly in summer. Glaciers at high altitudes and in polar regions can experience accumulation in any season.

The retreat of mountain glaciers is one of the most visible examples of climate change. A compilation of observations made by the World Glacier Monitoring Service on 19 regions around the world, gathering more than 40,000 observations shows that the retreat is an almost global phenomenon, despite some intermittent readvances related to dynamical instabilities (e.g. Island, Svalbard) or to specific climatic conditions (i.e. increased winter snowfall) observed on a few individual glaciers in Scandinavia or New Zealand in the 1990s. However, the periods of glacier front advances are short compared to the overall ice retreat. By compiling the data obtained on 169 glaciers since 1700, Oerlemans (2005) shows that the retreat of glacier fronts began in the 19th century, and accelerated strongly from 1850 onwards, with a continuation throughout the 20th century and early decades of the 21st century.

Regional analyses have shown that, until around 2000, the average mass balance cumulated over all European glaciers was close to zero, with significant mass losses for Alpine glaciers being compensated for by advances of glaciers in western Norway stemming from a sharp increase in precipitation in response to a positive phase of the North Atlantic Oscillation. From the year 2000 onwards, the Norwegian glaciers began to retreat in response to a decrease in precipitation. Over the period 2003-2009, the most negative mass balances occurred for glaciers in the northwestern United States and southwestern Canada, Central Europe, Southern Andes and low latitude areas. In the Alps, glaciers have been retreating since the mid-nineteenth century. In Switzerland, they currently cover only 60% of the area they occupied in 1850. Due to the heat wave, an exceptionally high loss of mass occurred in 2003, corresponding to a reduction of $2500 \text{ kg m}^{-2} \text{ yr}^{-1}$ for the nine glaciers studied. This value exceeds the previous record $1600 \text{ kg m}^{-2} \text{ yr}^{-1}$ in 1996 and is four times higher than the average measured between 1980 and 2001 ($600 \text{ kg m}^{-2} \text{ yr}^{-1}$). In Africa, the glacier area at the top of Kilimanjaro is now only 20% of what it was at the beginning of the 20th century. In Patagonia, the 'icefields' have lost between 3 and 13 km^3/yr of ice since the 1970s. The retreat of the glaciers in Nepal and Himalayas seems to have accelerated over the past twenty years, and in Tibet, the number of glaciers in retreat has recently multiplied.

The Fifth IPCC Assessment Report estimated that the contribution of glaciers and small ice caps to sea level rise over the 1993-2010 period was about 0.76 mm/yr (IPCC, 2013). Since then, new estimates based on new data indicate a higher contribution, demonstrating that mass loss from

glaciers and small ice caps has accelerated significantly since the early 1990s, and currently contributes between 1.05 and 1.12 mm/yr to the rise of the global sea level.

10.1.6.5 Polar ice sheets

Polar ice sheets are huge masses of ice formed, like glaciers, by continual accumulation of snow in excess of ablation, which gradually turns into ice under the effect of compaction. As for glaciers, this transformation occurs in a transition zone about one hundred meters thick called firn. Currently, the ice sheets are located at high latitudes, one near the North Pole, Greenland, the other centered on the South Pole, Antarctica. The area of the Greenland ice sheet is about $1.8 \times 10^6 \text{ km}^2$. In the center, the ice thickness is greater than 3000 m. The Greenland ice volume ($\sim 3.0 \times 10^6 \text{ km}^3$) represents about 10% of the worldwide freshwater supplies. Antarctica is composed of two effectively distinct ice sheets in the east and west, separated by the Transantarctic Mountains. Its ice volume is close to $27 \times 10^6 \text{ km}^3$ and its surface, almost 98% covered by ice, is about $14 \times 10^6 \text{ km}^2$. A large part of the western ice sheet lies below sea level. The West Antarctic ice sheet extends locally over the sea to form floating ice shelves, mainly in the embayments of the coast, as in the Weddell and Ross Seas. In contrast, East Antarctica, which is larger, rests largely on bedrock. It forms a plateau with an area exceeding $10 \times 10^6 \text{ km}^2$ covered by a large ice layer of more than 4000 m thick in the center.

The evolution of the part of an ice sheet grounded on the bedrock depends on its surface mass balance and its flow due to the deformation of the ice itself. When the temperature is high enough, the ice melts at the surface. As for glaciers, the surface mass balance is determined by the difference between accumulation and ablation. In addition, under the effect of its own weight, the ice flows by plastic deformation along the line of steeper slope, as well as by sliding on the bedrock when the local temperature is close to the melting point: this is called basal sliding. As ice is an insulating material, a temperature gradient is established between the colder surface and the warmer base. Furthermore, by changing the ice viscosity, the temperature also affects the flow velocities from the surface to the base of the ice sheet. Thus, the processes involved in the deformation of the ice are not the same at the surface and at the base of the ice sheet.

In the case of the Antarctic ice sheet, the surface temperature generally remains low enough so that ablation is negligible. The ice then drains into the ocean or feeds the floating ice shelves through ice streams characterized by a rapid outflow (i.e. low basal friction). The sources of these ice streams are found far upstream, and their contribution to the evacuation of grounded ice from the center of the ice sheet towards the edges is estimated at nearly 90%. The flow regime through the ice shelves is very different from that of grounded ice. In fact, whereas grounded ice is characterized by a shear regime in the vertical plane, the predominant constraints on the ice shelves are the horizontal shear and the pressure forces exerted by the sea. The destabilization of these glacial platforms is due to the increase in sea level, but also to the basal melting beneath the platforms. This melting is therefore related to the ocean temperatures under the ice shelves and to the energy released by ocean currents. The dislocation of these glacial plateaus leads to the formation of icebergs (i.e. ice calving). This is exactly what happened with the dislocation of the Larsen B ice shelf in 2002 which resulted in a surface loss of about 3250 km^2 . This could also occur in the coming years with the break-up of the Larsen C ice shelf in July 2017 (6000 km^2 of surface loss) and the continuous acceleration of the Twaithes glacier reported by satellite

observations since 1992. Moreover, as the ice-shelves exert a buttressing effect for the upstream grounded ice, their disintegration can cause the destabilization of a large part of the ice sheet.

There are different methods to measure the amount of ice stored in an ice sheet:

- a) **The measurement of inflow** (snow accumulation) **and outflow** (ablation, discharges to the ocean). Snow accumulation is often estimated from annual layers in ice cores and interpolated between different drilling sites. The use of high resolution atmospheric models is also becoming more common. Discharges of ice to the ocean are estimated from seismic or radar measurements of the ice thickness and from measurements of ice flow velocity. Ablation is usually determined from ice models forced with atmospheric reanalyses, climatology or outputs from global climate models calibrated with surface observations. The loss of mass beneath the ice shelves, this remains very difficult to quantify. In general, inflows and outflows cannot be estimated with a margin error of less than 5%, which implies uncertainties of 40 and 140 Gt/yr on the estimate of the mass balance of Greenland and Antarctica respectively.
- b) **Remote-sensing techniques.** These include altimetry measurements from radio-echo sounding, interferometry and gravimetry. Interferometry provides information on ice flow velocities. The altimetric measurements provide information on the spatial and temporal variations of the topography, which makes it possible to trace the ice volume variations, after correcting for the altitude of the bedrock and for variations in the thickness and density of the firn. In addition, these measurements are strongly dependent on the nature of the terrain (flat, sloping or hilly surfaces) and the snow surface conditions (density, viscosity, etc.) and this may, in some cases, make interpretation difficult. Finally, satellite measurements of the gravity field provide, for the first time, estimates of the ice mass changes. However, there are still significant uncertainties, especially regarding the cause of the change in mass, as this could come from the ice sheet itself, the air column, the evolution of the subglacial bedrock or even from masses near the ice sheet (i.e. ocean mass, masses of water or snow contained on nearby continents). These different effects are evaluated and then corrected, but a significant uncertainty remains, mainly how to correct for the altitude of the underlying Antarctic bedrock. Other sources of uncertainty relating to satellite measurements come from the fact that they do not provide complete coverage of the ice sheets. Moreover, in Greenland, for example, remote sensing techniques may underestimate the extent of the ablation area and the increased rainfall over some parts of the ice sheet during rainfall events.

Past published estimates of Greenland and Antarctic ice sheets obtained with these methods have often diverged. This was due to the way in which the different sources of uncertainty were estimated and to the fact that the different measurements did not cover the same regions and time periods. Within the IMBIE framework (Ice-sheet Mass Balance Intercomparison Exercise), scientists made a huge effort to combine, over common survey periods and common regions, various observations from satellite geodetic techniques (altimetry, interferometry, radio-echo sounding and gravimetry) with simulated surface mass balance estimates inferred from regional atmospheric models. This allowed for a reconciliation of the apparent disparities between the different methods and for a consistent picture of ice-sheet mass balance to be created (Shepherd *et al.*, 2012).

For Greenland, this compilation effort confirmed with a high confidence level that the ice sheet is continuously losing mass and that this process now affects all sectors of the ice sheet (Fig. 10a-

c). However, after a record mass loss in summer 2012, Greenland has seen a slight decrease in the short-term mass loss trend. The mass loss is partitioned between surface melting and dynamic ice discharges. Shepherd *et al.*, (2012) estimate that the ice mass loss is about -142 ± 49 Gt/yr over the IMBIE time period (1992-2011) with an acceleration of the mass loss rate as illustrated by the comparison between the estimations made for 1992-2000 (-51 ± 65 Gt/yr) and 2005-2010 (-263 ± 30 Gt/yr). Using gravimetry observations, Velicogna *et al.*, (2014) provide for a more recent estimate of the Greenland ice sheet mass loss for the 2003-2013 decade of 280 ± 58 Gt/yr with an acceleration in the loss rate bringing it to 25.4 ± 58 Gt/yr².

The case of the Antarctic ice sheet (Fig. 10.6b) is a bit different since recent observations have shown that mass loss was mainly driven by dynamic ice discharge resulting from enhanced ice flow of marine-terminating glaciers. The main region experiencing mass loss is the West Antarctic ice sheet (WAIS), especially in the Amundsen/Bellingshausen Sea sectors (e.g. Thwaites and Pine Island glaciers) and, to a lesser extent, the Antarctic Peninsula. According to a recent update of the IMBIE estimates (IMBIE team, 2018), the mass loss from the Amundsen and Bellingshausen Sea sectors increased from 53 ± 29 Gt/yr to 159 ± 26 Gt/yr over the 1992-2017 period, and from 7 ± 13 Gt/yr to 33 ± 16 Gt/yr in the Antarctic Peninsula. It has long been considered that the East Antarctic ice sheet (EAIS) was gaining mass due to enhanced precipitation, despite no firm consensus being established (Velicogna and Wahr, 2006; Ramillien *et al.*, 2006). However, recent estimates suggest that some sectors, such as the Wilkes Land region, are losing mass. As a result, the rate of change in ice-sheet mass is estimated to be $+11 \pm 58$ Gt/yr in 1992 (mass gain) and -28 ± 30 Gt/yr (mass loss) in 2017 (IMBIE team, 2018). Using a different technique, Rignot *et al.*, (2019) estimate an even larger mass loss from EAIS with a strongly reduced uncertainty.

Overall, taking the Antarctic and Greenland ice sheets together, it appears that mass losses have accelerated in recent years. This trend is correlated with an increase in surface ablation due to increasing temperatures, but also with an acceleration of ice flow and subsequent dynamic ice discharges.

Several processes are at the origin of ice mass loss. The increasing surface ablation, mainly observed in Greenland, is a direct response to increased atmospheric temperatures. However, the ocean warming also plays a key role. As oceanic temperatures rise, basal melting under the ice shelves is enhanced. Eventually, this may lead to the dislocation of ice shelves and to the removal of the buttressing effect mentioned above. This causes an inland retreat of the grounding line (i.e. the limit beyond which ice starts to float), and subsequently, an acceleration of the upstream grounded ice. Theoretically, this process is only valid for ice-shelves confined within their embayment. It is responsible for more than half of the ice mass loss at the margins of the Antarctic ice sheet. For unconfined ice shelves, another process, known as the Marine Ice Sheet Instability, may also apply. For a marine-based ice sheet, such as the WAIS, bedrock is often more depressed in the center of the ice sheet than it is at the margins. As ice flux increases with ice thickness, the position of the grounding line becomes highly unstable in areas of reverse bed slopes, and any change in ice thickness in the vicinity of the grounding line creates an irreversible retreat of the grounding line position. A second hypothesis is the lubrication of the subglacial substratum caused by meltwater produced at the surface that percolates to the base of the ice sheet. A third process that may be responsible for ice flow acceleration is hydro-fracturing (DeConto and Pollard, 2016). This mechanism is related to water coming from melting at the surface of the ice-shelf that may percolate inside the ice-shelves. Crevasses can form and widen when the water pressure is high

enough, thereby favoring iceberg calving. Ultimately, this process may lead to ice-shelf collapse. It may also favor the marine ice sheet instability. Indeed, once the ice shelves have collapsed, ice cliffs become unstable and fall down if their height is greater than ~90 m. However, this process remains poorly constrained and is still a matter of debate.

A special attention is given to the evolution of ice sheets. Indeed, ice sheets strongly interact with the other components of the climate system. These interactions can lead to a highly non-linear climate response. This means that the effects of the radiative disturbance (caused by variations in insolation or in the amount of greenhouse gas in the atmosphere) can be amplified or mitigated by these feedback processes, as illustrated in Chapter 8 for abrupt events. Many studies on these interactions have been published over the past two decades. They would deserve a full chapter. Here, we only give some quick examples for time scales ranging from a few decades to a few centuries. Ice sheet melting is first of all accompanied by possible changes in albedo and therefore in the surface energy balance. This effect is almost instantaneous. In turn, a change in the energy balance can lead to changes in the mass balance of the ice sheets. Another consequence of the melting and/or mechanical destabilization of the ice sheets, widely discussed in the literature, concerns the freshwater flux release in the ocean. Locally, this release leads to a decrease in ocean surface temperatures, a change in sea ice cover and a reduction of ocean density in the vicinity of the ice sheets. Density changes also cause a disruption of large-scale ocean circulation by altering deep-water convection. For example, meltwater from Greenland has the potential to weaken the Atlantic Meridional Overturning Circulation. These changes can have effects in regions far from the polar zones. For example, the recent study by DeFrance *et al* (2017) showed that for a substantial melting of Greenland under a climate change driven by the RCP8.5 scenario, Greenland meltwater could cause a massive alteration of the monsoon regime with a drastic decrease in West African rainfall, and subsequently with a significant reduction in cultivable areas. Therefore, in addition to the direct and obvious consequences on sea level, the future of polar ice sheets is of primary importance for the future of human societies, all the more so if they are already economically fragile.

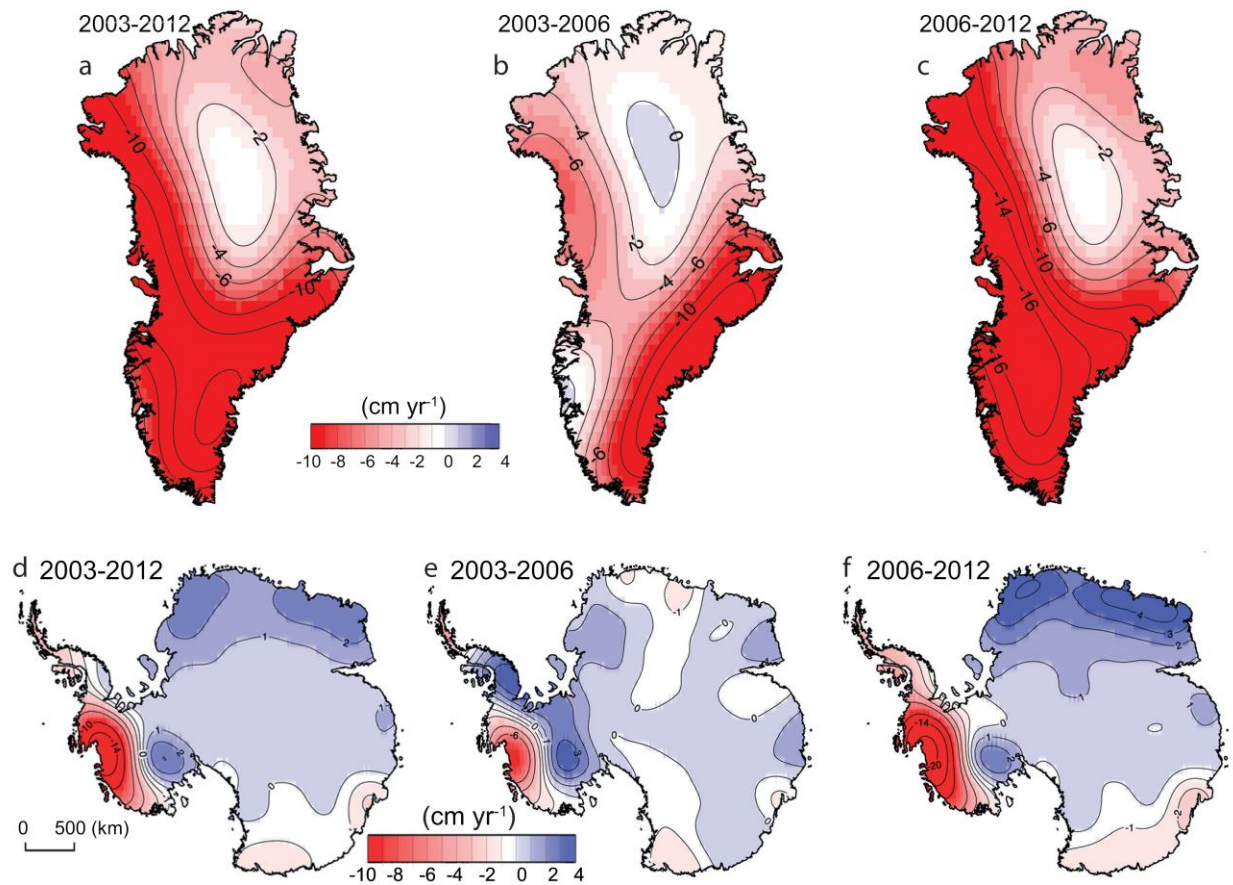


Fig. 10.6: Temporal evolution of ice loss in Greenland (top) and Antarctica (bottom) determined from time variable gravimetry observations from the GRACE satellite, shown in centimeters of water per year for the periods 2003–2012, 2003–2006 and 2006–2012, color coded red (loss) to blue (gain) (Source: IPCC, 2013).

10.1.7 Sea level changes

Sea level variations are the result of changes in both the volume of the oceans and ocean basins, as well as in the mass of water contained in the oceans. Depending on the time scale being considered, these types of variations have different origins. Over geological time scales, changes in the shape of ocean basins and in the continent/ocean distribution are the main factors affecting sea level. Over glacial-interglacial cycles, sea-level variations are mainly related to changes in continental ice volume and to the isostatic adjustment due to the vertical movements of the Earth's crust in response to changes in the mass of land ice. Following the last deglaciation initiated about 21,000 years ago, sea level rose by ~120 m and then stabilized around 6,000 years ago. Geological data indicate that sea level has not changed by more than 30 cm from that time until the end of the 19th century.

On time scales ranging from a few years to a few decades, variations in the mean sea level are the result of two factors, mainly related to climate change:

- a) Variation of the ocean volume caused by changes in sea temperature. As temperature increases, the volume of water expands. This process is called thermal expansion;
- (b) Variations in the bodies of oceanic water resulting mainly from exchanges with continental reservoirs, such as rivers, lakes and inland seas, snowpack, ground water, but also mountain glaciers and polar ice sheets.

Other factors such as ocean circulation or atmospheric pressure can bring about local variations, without altering the mean global sea level. In addition, some human interventions have the effect of modifying regional hydrology by modifying the runoff of freshwater released to the ocean, and thus the sea level. This occurs in the case of dams, irrigation, urbanization, water extraction from aquifers and deforestation. Some of these processes have the effect of increasing runoff (urbanization, deforestation); others, such as dams and irrigation, contribute to the sequestration of freshwater on the continents. Current estimates of the net land water storage are made based on observations and models, and vary between -0.33 to 0.23 mm/yr over the period 2002–2014/15 (WCRP Global Sea Level Budget Group, 2018).

Measurements of current sea-level variations are based on two different techniques: tide gauges, which began to be installed in the 19th century, and altimetry data from satellite observations since 1992. The two main limitations of tide gauges are their inhomogeneous spatial and temporal coverage, and the inclusion of vertical land motion in their record, which needs to be corrected for to obtain relative sea-level changes. To limit the uncertainties related to these movements, which are difficult to quantify in current models, only a few tens of geologically stable sites, mainly located along the coasts of North America and Europe, are taken into account to inform us of the sea level evolution in the course of the 20th century. Based on a compilation of the most recent estimates, the sea-level rise as indicated by tide gauge data is estimated at 1.7 ± 0.2 mm/yr between 1901 and 2010 for a total sea level rise of 0.19 ± 0.02 m (IPCC, 2013).

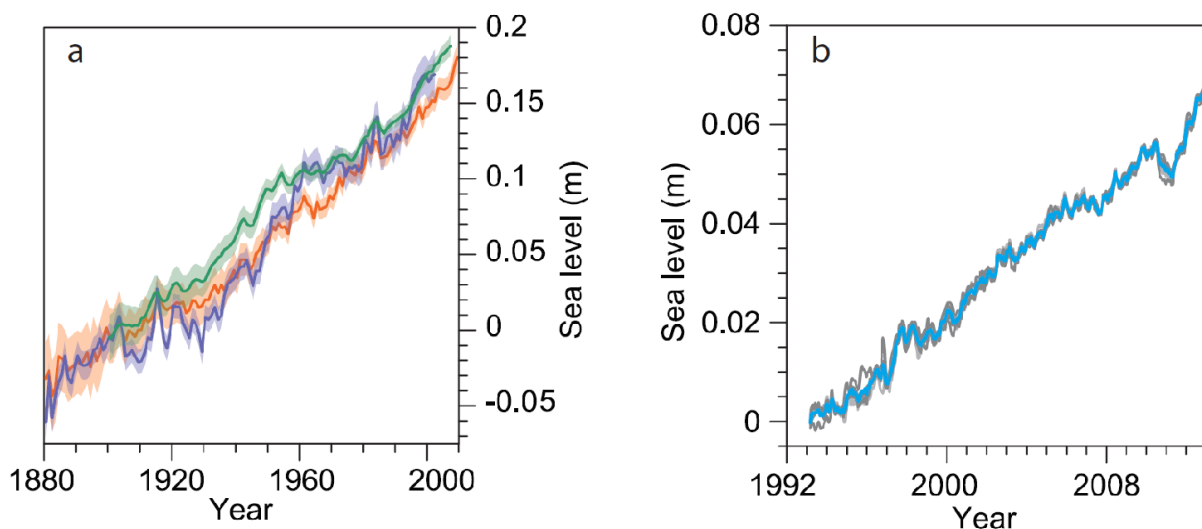


Fig. 10.7: (a) Yearly average global mean sea level (GMSL) reconstructed from tide gauges by three

different approaches: orange from Church and White (2011), blue from Jevrejeva *et al.*, (2008), green from Ray and Douglas (2011), (b) Changes in the mean global sea level from altimetry data sets from five groups (University of Colorado (CU), National Oceanic and Atmospheric Administration (NOAA), Goddard Space Flight Centre (GSFC), Archiving, Validation and Interpretation of Satellite Oceanographic (AVISO), Commonwealth Scientific and Industrial Research Organisation (CSIRO) with the mean of the five shown as a bright blue line (Source: IPCC, 2013).

Since 1992 and the launch of the TOPEX/Poseidon satellite, altimetric data have provided a new way of estimating sea-level variations, based on the time required for the round trip of the radar wave and on the satellite altitude defined above a standard reference surface. These measurements are thus independent on the vertical land motion, in spite of a small correction (around 0.3 mm/year) to account for the change in the reference level at the ocean bottom due to the post-glacial rebound (Peltier, 2015). This results in an increase of about 3.2 ± 0.4 mm/yr between 1993 and 2012 (IPCC, 2013, Figure 10.7), now reevaluated at 3.1 ± 0.4 mm/yr between 1993 and 2017 (WCRP Global Sea Level Budget Group, 2018). Satellite altimetry data now cover a time period of 25 years, long enough to identify an acceleration of the sea level rise estimated at around 0.084 ± 0.025 mm/yr² (Nerem *et al.*, 2018).

These altimetry data show significant regional disparity, with some regions showing a sea-level rise well above the global mean and other regions showing a decrease in sea level. This regional variability partially explains the differences between tide gauge data and altimetry data, and is due to several factors including density variations, ocean circulation, atmospheric pressure, and variations within the solid Earth or geoid. For example, the Scandinavian shield continues to rise at a faster rate than the mean and, so paradoxically, a decrease in local sea level is recorded there.

Tide gauges and altimetry data provide ways of quantifying the global mean sea level rise and its different components. Data on ocean temperature changes allow us to quantify the contribution from thermal expansion. Recent advances in temperature measurements have greatly improved our knowledge. Since 2000, the Argo project has deployed thousands of free-drifting profiling floats measuring temperature (and salinity) in the ocean at depths between 0 and 2000 m, providing a continuous record of heat penetrating in the ocean. In addition, ship-based data were collected during the World Ocean Circulation Experiment, providing the means to estimate the deeper ocean temperature change (Johnson *et al.*, 2007; Purkey and Johnson, 2010; Kouketsu *et al.*, 2011). These data show that, globally, the ocean has warmed significantly over the last 50 years, and in particular, over the past two decades. By vertically integrating the temperature data along the water column at each oceanic point, sea-level changes due to oceanic thermal changes can be estimated over the past 50 years. Based on data gathered over a depth of 700 meters, the contribution of thermal expansion to sea level rise was estimated at 0.60 ± 0.2 mm/yr for the period 1971-2010 (0.8 ± 0.3 mm/yr if the deep ocean contribution is included). For the more recent period 1993-2017, this contribution is 1.3 ± 0.4 mm/yr (Table 10.1). In recent decades, this has been the dominant contribution to global sea level rise.

The other factors contributing to the rise in sea level come from changes in the oceanic water mass (Table 10.1). One of the most important contributions is from mountain glaciers (excluding Greenland and Antarctica) which cause a global sea level increase of 0.62 ± 0.37 mm/year for the period 1971-2010 and 0.65 ± 0.15 mm/year for the period 1993-2017. Both polar ice sheets also contribute to the recent rise in global sea level with 0.48 ± 0.10 mm/yr for Greenland and

0.25 ± 0.10 mm/ yr for Antarctica for 1993-2017. The ice-sheet contribution to sea-level rise has been increasing from 27 % of the total contributions for 1993-2017 to 40 % for 2005-2017.

The sum of all contributions, including land water storage, amounts to 2.8 ± 0.5 mm/yr for the period 1993-2010, which is lower than the observed global mean sea level rise of 3.2 ± 0.4 mm/yr (Table 10.1). Similarly, for the most recent period 2005-2017, the sum of contributions is 2.95 ± 0.21 mm/yr, lower than 3.5 ± 0.2 mm/yr which is the observed global mean sea level rise. This discrepancy is due to uncertainties in the estimation of the different components of ocean mass contributions (glaciers, ice sheets and land water storage). Instead, if the ocean mass contribution is taken from gravity measurements using GRACE (Gravity Recovery And Climate Experiment), the sum of thermal expansion and GRACE-based ocean mass contributions is 3.6 ± 0.4 mm/yr, which is in the error bar of the observed global mean sea level rise for this period (3.5 ± 0.2 mm/yr).

Components	Sea level rise (mm/yr)	Sea level rise (mm/yr)	Sea level rise (mm/yr)
	1993-2010 (IPCC, 2013)	1993-2017 (WCRP Global Sea Level Budget Group, 2018)	2005-2017 (WCRP Global Sea Level Budget Group, 2018)
1. Thermal expansion	1.1 ± 0.2	1.3 ± 0.4 (48 %)	1.3 ± 0.4 (44 %)
2. Glaciers (excluding Greenland and Antarctica)	0.76 ± 0.37	0.65 ± 0.15 (24 %)	0.74 ± 0.1 (25 %)
3. Greenland ice sheet	0.33 ± 0.08	0.48 ± 0.10 (18 %)	0.76 ± 0.1 (26 %)
4. Antarctic ice-sheet	0.27 ± 0.11	0.25 ± 0.10 (9 %)	0.42 ± 0.1 (14 %)
5. Land water storage	0.38 ± 0.11	/	-0.27 ± 0.15 (-9 %)
Total of contributions (1+2+3+4+5)	2.8 ± 0.5	2.7 ± 0.23	2.95 ± 0.21
Observed global mean sea level rise	3.2 ± 0.4	3.07 ± 0.37	3.5 ± 0.2
Thermal expansion + GRACE-based ocean mass			3.6 ± 0.4

Table 10.1: Sea level rise from different sources, adapted from IPCC (2013), Chapter 13, with additional data from WCRP Global Sea Level Budget Group (2018). The percentages are relative to the sum of contributions.

10.2 Climate modeling and recent changes

10.2.1 Simple radiative climate models and their limitations

To estimate the changes in the mean Earth's temperature in response to different radiative forcings (solar irradiance, greenhouse gases, energy re-emitted by the surface etc.), a first approach is to use purely radiative models. With these models, one can easily and accurately calculate the temperature changes with some simplifications: it is assumed that only the temperatures change, and that this affects only the radiation emission law, without modifying any radiative property of the atmosphere or the surface. With a doubling of atmospheric CO₂ concentration, for example, a temperature increase of $1.2 \pm 0.1^\circ\text{C}$ is obtained. However, these simplified assumptions are not reliable, because when the temperature changes, all the other climate variables (e.g. humidity, wind, clouds, rain, snow cover) also change. These changes can in turn modify the energy balance of the surface and the atmosphere and thus have an additional effect on temperatures. These are called *feedback processes*. They are said to be positive when they have they amplify the initial disturbances, and are said to be negative when the opposite is true, where they work towards the stabilization of the system.

The first studies which took these feedbacks into account were carried out using radiative-convective models, with only one vertical dimension. For example, Manabe and Wetherald (1967) showed with their model, that the surface warming due to a doubling of the atmospheric CO₂ concentration was 1.3°C when the absolute humidity of the atmosphere remained constant, but reached 2.4°C in case of constant relative humidity. Numerous other studies have confirmed the crucial importance of feedback mechanisms on the magnitude of global warming: they can amplify twice to four times the temperature variation compared to the situation where no feedback is taken into account. These studies have also shown that the magnitude of these feedbacks is strongly dependent on complex physical processes (less understood than radiative transfer), such as turbulence, convection, cloud formation and precipitation (Ramanathan and Coakley, 1978). These processes, and in particular, the atmospheric circulation which determines how energy and water vapor are redistributed within the atmosphere, cannot be represented in a useful way in the radiative-convective models. Thus, even rough estimates of the changes in the global mean temperature require the atmospheric dynamics to be taken into consideration and, for more precise calculations, three-dimensional models representing the general circulation of the global atmosphere of the Earth need to be applied.

10.2.2 General Circulation Models: progress and limitations

10.2.2.1 The evolution of climate models

A general circulation climate model is a simplified representation of the climate system, but including as best as possible most processes that influence the climate. It is based on a preliminary physical analysis, in order to reduce the number of processes to be incorporated, as well as on appropriate mathematical and numerical formulations. Numerical modeling of the climate began in the 1970s and has since greatly progressed, thanks to the steady increase in the processing power of computers. The general philosophy behind this development, established by Charney and his

collaborators in the 1950s, was to understand the problem on a global scale, even if this meant making very general approximations initially, with the aim of gradually improving the model by identifying its drawbacks and its limitations. The first models only described the atmosphere and the continental surfaces. In order to reduce model complexity, the oceanic surface temperature was imposed: even if the energy balance of the ocean surface is very different from the observed measurement, the surface temperature is maintained at its prescribed value. However, to investigate the variations in climate accounting for oceanic temperatures is required.

The first studies of the impact of a CO₂ doubling using this type of model were carried out in the 1970s at the GFDL (Geophysical Fluid Dynamics Laboratory, Princeton, USA) with a representation of the ocean with no circulation and zero heat capacity, so that equilibrium could be achieved quickly. In this model, there was no diurnal or annual variation in insolation, and ad hoc corrections were applied to heat fluxes at the air-sea interface to keep the ocean surface temperature close to observations. The use of this type of model became widespread during the 1980s, with a gradual increase in sophistication and realism. For example, both annual and diurnal insolation variations were incorporated, modeling of cloud formation processes began, etc. At the same time, new satellites were being used to estimate global cloud cover and radiative fluxes at the top of the atmosphere, which contributed to the improvement and evaluation of atmospheric models.

In parallel, ocean general circulation models were developed to simulate heat transport and to study the role of the ocean in the Earth's energy balance. Progressively, they included sea-ice models and, from the 1990s onwards, they were coupled with atmospheric models to simulate the atmosphere-ocean-sea ice interactions. These early models did not simulate the heat and water fluxes at the air-sea interface, resulting in strong biases in the simulated oceanic surface temperatures. To fix these shortcomings, the fluxes at the air-sea interface were corrected in an ad hoc, before these corrections were gradually removed after the end of the 1990s, thanks to continuous model improvement.

These coupled atmosphere-ocean models gradually became the basic tool for studying both past and future climate variations. For example, in preparation for the Fourth IPCC Assessment Report (IPCC, 2007), some twenty of these coupled models performed a whole series of climate change simulations, and only six of them were based on flux correction at the air-sea interface. These models can simulate a natural climate variability that can then be compared to observations at different time scales: a few days, a few years (interannual variability, the best known of which is El Niño), or a few tens, or even several hundred years.

In a schematic way, climate models simulate the energy and water cycles. Progressively, representations of chemical reactions in the atmosphere, biogeochemical cycles and the transport of species were introduced into modeling so as to study new aspects of climate variations: the effect of aerosols, coupling between climate change and the chemical composition of the atmosphere, and between climate change and the carbon and methane cycles. This required advances in our understanding of each of the components of the system: atmosphere, ocean, vegetation, continental surface, sea ice. Numerical climate models progressively incorporate, in a coherent way, a wide range of physical processes governing the climate variations and the interactions between the different climate components. On the other hand, the inclusion of a growing number of physical processes has made the models more complex and more difficult to develop and evaluate.

As ice sheets interact with atmosphere, ocean and vegetation, the next key challenge for the climate modeling community is to incorporate ice-sheet models in general circulation climate models. This is a necessary step to obtain a comprehensive representation of the climate system for past, present and future time periods.

10.2.2.2 What are the uncertainties inherent in climate models?

The climate is characterized by a very wide range of both spatial (from the micrometer to several thousand kilometers) and temporal (from the second to several thousand years or more) scales. The processes at these different scales interact with one another, and in principle, it is never possible to know which scales should be considered and how to represent the neglected scales in a simplified way. A typical example is the formation of clouds and precipitation. Let's take the example of convective clouds (of the cumulonimbus type), whose core is a rising column of moist air in which the water vapor condenses as it rises. This ascending column mixes with the surrounding drier air, and this mixing depends on many factors (for example, the intensity of the upward thermal current and wind shear). In order to take these mixtures into account, it is first necessary to know precisely the vertical profile of the atmospheric variables in the vicinity of the column. The turbulent exchanges between the column and its environment must also be calculated, as well as the coupling between these turbulent exchanges and the formation or dissipation of rain drops, hail or snowflakes. This requires a modeling on a very small scale (a few hundred nanometers to a few meters), which is not possible with global models. Therefore, a simplified model must be developed based only on large scale variables which reproduce the effect of unresolved small scale processes. This type of modeling, called parameterization, is based on important simplifications that nevertheless require a thorough physical analysis and an in-depth understanding of the phenomena. The aim is to obtain a simplified model that is not only as accurate as possible, but also justified and well understood.

There are many parameterizations in a climate model which can have direct connections with the atmospheric circulation (for example gravity waves and orographic effects), the calculation of the exchanges by radiation, deep convection, or boundary layer phenomena. Many of these parameterizations play a key role in the water cycle, the formation of clouds and their radiative properties, precipitation, heat and water fluxes on the surfaces of continents or oceans, among others. All these phenomena have an impact on the simulation of the current climate and as there are strong interactions between them, it is often very difficult to identify the precise role of each of the parameterizations on the simulation of these phenomena, and in particular to understand why some of them are poorly simulated.

Parameterizations also play a very important role in the climate response to different forcings, and in the simulation of past and future climate changes. One example is the simulation of clouds. Clouds exert two opposing effects on the terrestrial radiative balance: on the one hand, they reflect part of the solar radiation, and on the other, they absorb infrared radiation and thus contribute to the greenhouse effect. The relative importance of these two effects depends on many factors, in particular, cloud altitude. Over the past twenty years, we have learned that, on average, the first effect outweighs the second, and therefore that clouds have a cooling effect on the climate - especially low-lying clouds, because they have little impact on infrared radiation. However, this does not explain the role that clouds could play in global warming. Depending on how their properties change, clouds may attenuate or, on the contrary, amplify, global warming. The physical

formation mechanisms involve so many processes and spatial scales (from a micrometer to a thousand kilometers), and their radiative properties depend on so many factors that it is impossible to conclude on the basis of theory, simple reasoning or analysis of available observations, how they will evolve in the future.

10.2.3 Simulation of the current climate and recent changes

Analysis of simulated climate combined to the comparison of model results with observations is an important step to establish the reliability of climate models. The aim is to evaluate not only the mean climate, but also the climate variability at different time scales (from a few days to a few decades) as well as recent climate changes. Unless otherwise indicated, this section presents the simulated climate characteristics from the twenty AOGCMs that contributed to the preparation of the Fifth IPCC Assessment Report (IPCC, 2013).

10.2.3.1 Mean climate

The difference in mean insolation is what causes the temperature difference between the equator and the poles. This difference is the main driver of atmospheric and oceanic circulations, which act to reduce the equator-pole temperature gradient. It is also influenced by the presence of clouds, reflective surfaces (snow, glaciers, sea ice), large mountain ranges and the topography of the ocean. Latitudinal temperature variations are thus a key criterion for evaluation of climate models. All the models simulate this strong equator-pole gradient: the simulated temperature is 25°C at the equator, -20°C at the North Pole and -40°C at the South Pole, which agrees with observations. However, the models also show significant biases over Antarctica, Greenland, and over large mountain ranges in general, such as the Himalayas. These are due to an approximate representation of the topography (due to the limited spatial resolution of the models) and a poor representation of turbulent exchanges under conditions of strong thermal stability. Over the oceans, there is a warm bias on the eastern coasts caused by a poor representation of stratus clouds observed in these regions.

The annual variation in solar radiation is the strongest energy ‘disruption’, apart from the diurnal cycle, to which the surface of the Earth is subjected. The observed seasonal temperature cycle is generally well reproduced by the models: it is higher at high latitudes than at low ones (30°C vs. 5°C, essentially reflecting the seasonal amplitude of incoming solar radiation), and is higher over continental areas than above the oceans, mainly because of the lower thermal inertia of the continents.

The formation of precipitation involves numerous processes, some of them on a small scale, and remains one of the phenomena that models have the largest difficulties in correctly simulating. Around the equator, the area of maximum precipitation, corresponding to the intertropical convergence zone, is well simulated by the models (Fig. 10.8). In the Pacific Ocean, observations show that the maximum is at 10°N, indicating that this convergence zone is located mainly in the northern hemisphere. The models, on the contrary, generally have two maxima located on either side of the equator, the southern maximum extending almost to the coasts of Peru, although observations indicate that precipitation is almost absent in this region. In observations, the maximum rainfall ranges from northern New Guinea to southern South America. On the

continents, one of the biggest flaws of the models is that the intensity of rainfall over the Amazon is too low.

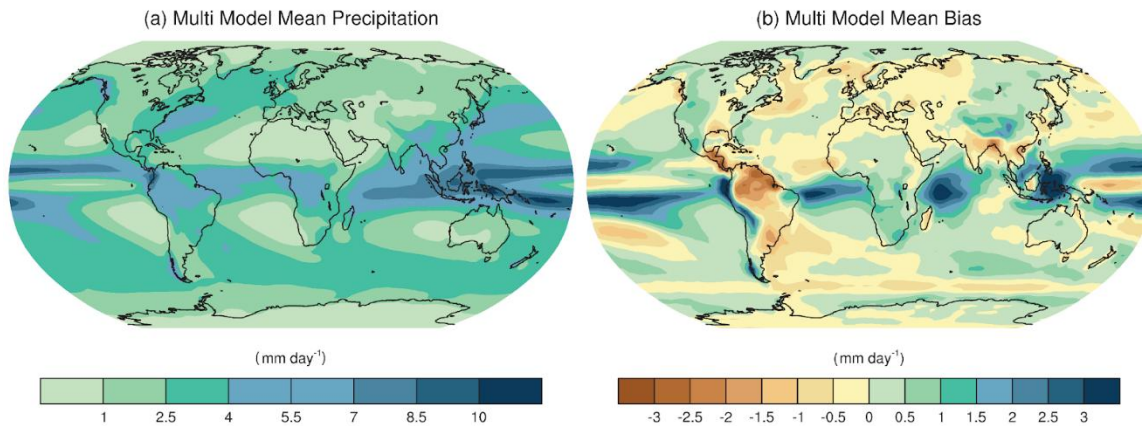


Fig. 10.8: Annual-mean precipitation rate (mm/day) for the 1980–2005 period. (a) Multi-model-mean constructed with one realization of all available AOGCMs used in the CMIP5 (Coupled Models Intercomparison Project, Phase 5) historical experiment. (b) Difference between multi-model mean and precipitation analyses from the Global Precipitation Climatology Project (Adler *et al.*; 2003) (Source: IPCC, 2013).

The extent and characteristics of sea ice are relatively well simulated by current models, both in terms of mean value and seasonal cycle. However, in the Arctic basin, few models are able to successfully replicate the distribution of sea ice thickness, which should be less than 1 m north of Siberia, to more than 5 m north of Greenland and of the Canadian archipelago. This difference in ice thickness is mainly due to winds, which move ice from the Siberian coasts to Canadian shores and Greenland. These winds allowed FRAM, the F. Nansen’s boat, to cross the Arctic Ocean at the end of the 19th century although it was trapped in the ice. The spatial distribution of ice thickness is generally poorly simulated by the models due mainly to poorly simulated surface winds.

10.2.3.2 Climate variability

The mean climate state gives a very incomplete picture of the climate. Indeed, climate varies continuously over a very wide range of space and time scales with fluctuations having hourly, daily, interannual, decadal or even longer time scales.

One way to characterize these fluctuations is to select those having a large-scale spatial structure (typically, the scale of an ocean basin or a continent), whether fixed or spreading, and to characterize its temporal evolution (amplitude, phase). To describe these fluctuations, we refer to what we call *modes of variability*. Some of which are well known, such as the El Niño-Southern Oscillation (ENSO) in the tropical Pacific or the North Atlantic Oscillation (NAO), which dominates the weather and climate fluctuations over Europe.

ENSO is the dominant mode of tropical variability at the interannual to decadal time scale. The warm phase, or the El Niño event, is characterized by a warming of the eastern tropical Pacific (along the equatorial cold water tongue) and an easterly displacement of the zone of maximum

precipitation, usually located above Indonesia. The cold phase, or La Niña, is characterized by negative sea surface temperature anomalies (i.e. temperatures below the climatological mean) and can be interpreted as an enhancement of the seasonal climatological cycle. This mode of variability is a coupled ocean-atmosphere oscillation that affects atmospheric circulation throughout the tropical belt and ocean circulation throughout the Indo-Pacific basin. Its periodicity is between three and seven years, and the characteristics of ENSO events observed in the 20th century can vary considerably from one event to another. All current climate models simulate a mode of tropical variability with general characteristics resembling those of ENSO. This was not the case with the previous generation of climate models. Nevertheless, the spatial structure of these events is not generally well simulated, such as the asymmetry between the El Niño and La Niña episodes. In terms of the recurrence of these events, the periodicity simulated by the models is usually too short and too regular. In general, the strong diversity of observed spatial and temporal characteristics of ENSO is often poorly simulated. Research works are being done to identify the impact of the different atmospheric and oceanic processes on the characteristics of ENSO, and on the reasons for model errors.

The Madden and Julian - MJO - oscillation (Madden and Julian, 1994) is the main mode of intra-seasonal variability in the tropical region, with a periodicity of between 30 and 90 days. Unlike ENSO, whose spatial structure is stationary, this oscillation is characterized by a wave that propagates from west to east, the intensity of the convection alternating between reinforced and reduced. An MJO- type signal is present in the results of most models, but several essential characteristics of this mode of variability (amplitude, phase, propagation) are not realistic. The roles of the different processes and their interactions in the characteristics of this mode of coupled atmosphere-ocean variability have not been well identified and several hypotheses have been proposed.

In the extratropical regions, an important mode of variability is the North Atlantic Oscillation (NAO). It is a pressure oscillation between the temperate and the subpolar latitudes, often defined as the difference in normalized pressure between the Icelandic low and the Azores anticyclone. It is associated with changes in prevailing westerly winds throughout the North Atlantic Basin, and affects the climate of Europe and its surroundings. For example, the positive phases of NAO (NAO +) are associated with a northward shift of low pressure systems with mild and rainy winters and droughts in southern Europe. Current models correctly simulate the spatial properties of the NAO, but are not as good at simulating its temporal properties. In particular, the current trend of the NAO (an increase in positive phases) is underestimated by the models. The reasons for this underestimation are diverse: i/ the interactions between the stratosphere and the troposphere, ii/ the exchanges between stationary waves and transient activity (storms) and iii/ the exchanges with the surface of the ocean.

10.2.3.3 Recent evolution of the climate

Over the last 150 years, the evolution of the global surface temperature is documented with a large set of observations. Simulating this evolution is therefore one way to test climate models. Between 1850 and 2000 the steady increase in the concentration of greenhouse gases has led to an increase in radiative forcing of about 2.5 W/m^2 . The uncertainty in this forcing is estimated to be quite low at less than $\pm 10\%$. Since fossil fuels contain sulfur, CO_2 emissions are accompanied by

SO₂ emissions which lead to the formation of sulfate aerosols. In 2000, these aerosols produced a radiative forcing of about -1 W/m², but, depending on how it is estimated, this value varies from -0.5 to -2 W/m². In addition, other aerosols, such as soot or aerosols from biomass fires, may also play an important role, but their effects are even less well known. Thus, about a third of the positive radiative forcing (albeit with a high degree of uncertainty) from the increase in greenhouse gases is masked by the negative radiative forcing from aerosols. In addition to anthropogenic forcings, there are natural forcings. At the century time scale, aerosols are mainly injected into the stratosphere by variations in the intensity of incoming solar radiation, and by strong volcanic eruptions where they can remain for several months or even years. These aerosols reflect solar radiation, creating a negative forcing. At the end of the 20th century, strong volcanic eruptions were more frequent than at the beginning, resulting in an enhanced radiative forcing. Therefore, regardless of the climate response, there is already an inherent uncertainty in the radiative forcing of about ± 50% (IPCC, 2013).

When only natural forcings are considered, simulated warming is not in line with observations, especially since the 1980s (Fig. 10.9). However when all forcings are taken into account (natural + anthropogenic), all models are able to correctly simulate the increase in the mean Earth temperature over the past 150 years (Fig. 10.9). Models simulate a greater increase in temperature over the continents than over the ocean and a geographic distribution of warming in agreement with observations (IPCC, 2013). Thus, temperature changes over the past 150 years make it possible to verify that the climate response simulated by the models is coherent with the observed temperature variations, although there is too much uncertainty in the forcings to be able to constrain precisely the climate sensitivity of the models.

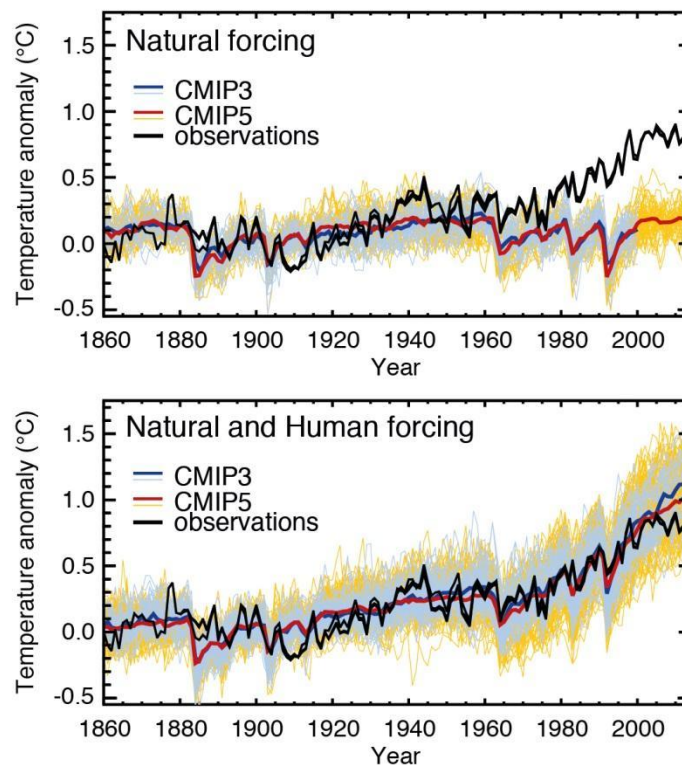


Fig. 10.9: Temporal evolution of the global air surface temperature of the Earth: observations (black line) model simulations taking only natural forcings into account (top), and taking both natural and anthropogenic forcings into account (bottom). The red and blue lines represent the multi-model average of the CMIP3 and CMIP5 (Coupled Models Intercomparison Project, Phases 3 and 5) models respectively (Source: IPCC, 2013).

The aerosols have two opposing effects: one warming the surface, the other cooling it. The first one, called the direct effect, is the diffusion of incoming solar radiation, where part of the solar radiation is returned to space. The second, the indirect effect, is the modification of the optical properties of clouds: the presence of a large number of aerosols increases the number of condensation nuclei. For the same amount of liquid water, more numerous drops forming the clouds tend to have a smaller radius and thus to diffuse more solar radiation. Aerosols are also likely to modify the formation of rain, and therefore the liquid water content of clouds. The complexity of the radiative properties of aerosols in the atmosphere make it more difficult to model the impact of cloud physics.

10.3 Projecting the future of the climate system

10.3.1 Climate response to a doubling of CO₂: forcings and feedbacks

Perturbations that modify the energy balance of the climate system are quantified in terms of energy flux at the top of the atmosphere. Quantifying the forcing due to a variation in average insolation is immediate. For a change in the greenhouse gas concentration, a radiative model is used to calculate how these changes affect fluxes at the top of the atmosphere. Since the late 1980s, it is now possible to perform these calculations using radiative transfer codes and spectral databases, provided that all other atmospheric (e.g. clouds, aerosols) and surface (e.g. snow cover) characteristics are assumed to be fixed. For a doubling of the atmospheric CO₂ concentration, the global mean annual radiative forcing at the top of the atmosphere is $3.7 \pm 0.2 \text{ W/m}^2$. As we focus on slow climate variations, the calculation of the radiative forcing takes into account the rapid adjustment of the stratospheric temperature.

In response to the radiative forcing ΔQ , the different climate models simulate a temperature change at equilibrium ΔT which is different from one model to another. These differences are difficult to analyze and interpret directly because of the high level of model complexity. A standard method to identify the origin of these differences is the feedback analysis (see, for example, Dufresne and Saint-Lu (2016)). From the temperature change at equilibrium ΔT , a ‘feedback parameter’ λ is defined:

$$\lambda = -\Delta Q/\Delta T.$$

By writing this equation in the form $\lambda \times \Delta T + \Delta Q = 0$, we see that $\lambda \times \Delta T$ represents the variation in the average flux at the top of the atmosphere necessary to compensate for the radiative forcing ΔQ . We can therefore write $\lambda = -dF/dT$, with F being the net radiative flux at the top of the atmosphere, counted as positive when it is descending. This derivative can be decomposed, in the first order, as a sum of partial derivatives:

$$\lambda = -\sum \partial F / \partial X \times \partial X / \partial T$$

The sum over X is the sum of all the X variables affecting the radiative balance at the top of the atmosphere and that are modified when the surface temperature changes. These are mainly the three-dimensional fields of temperature, water vapor and clouds, and the two-dimensional fields of surface albedo. The change in the temperature field is generally broken down into two terms, one corresponding to a uniform temperature change, the other to the non-uniform part of the temperature change. Finally, the parameter λ can be decomposed as follows:

$$\lambda = \lambda_P + \lambda_L + \lambda_c + \lambda_w + \lambda_a$$

The terms of the right-hand side are the respective feedback parameters: Planck λ_P (uniform temperature change), the temperature gradient λ_L (non-uniform part of the temperature change), clouds λ_c , water vapor λ_w and surface albedo λ_a .

These parameters are often calculated as follows using the partial radiative perturbation method. For a given climate model, two simulations are carried out, a reference one and a perturbed one. The fluxes at the top of the atmosphere are calculated off-line from the outputs of the reference simulation using a radiative code. They are then recalculated by replacing the values of some variables (temperature, humidity, clouds, surface albedo) from the reference simulation with the corresponding values from the perturbed simulation. The difference between these two fluxes gives the sensitivity of the fluxes at the top of the atmosphere to a perturbation of each of the variables.

The particular Planck parameter λ_P corresponds to the response of the flux at the top of the atmosphere to a uniform temperature change at the surface and within the whole atmosphere. Its value is approximately $-3.2 \text{ W/m}^2 \text{ K}$. There is very little change in this value from one model to another, and the sign convention used corresponds to a decrease in the Earth's energy balance when the surface temperature increases. In response to a radiative forcing, ΔQ , the surface temperature response can be calculated if the Planck parameter λ_P is the only non-zero feedback parameter:

$$T_P = -\Delta Q / \lambda_P .$$

This so-called Planck response causes an increase of 1.2°C for a forcing of 3.7 W/m^2 , resulting from a doubling of the CO_2 concentration. It is the response of an idealized system in which only the atmospheric and surface temperatures can change uniformly and where only the radiation emission law is affected (see section 10.2.1 of this chapter). It can be said that this is the response with no feedback from the climate system. By combining the above equations, the increase in temperature at equilibrium ΔT can be written as a function of the Planck response:

$$\Delta T = \Delta T_P / (1 - g)$$

where g is the feedback gain of the system:

$$g = -(\lambda_L + \lambda_c + \lambda_w + \lambda_a) / \lambda_P .$$

If the gain g is positive and less than 1, the feedbacks will amplify the temperature increase ΔT , relative to ΔT_P . Conversely, if the gain is negative, the ΔT increase will be attenuated. In the preparation of the Fifth IPCC Assessment Report (IPCC, 2013), climate change simulations were

conducted within the CMIP5 project by around forty climate models. In particular, for a doubling of the CO₂ concentration, the models simulate a global warming of 3°C on average (between 2.0 and 4.6°C depending on the model), until a new energy equilibrium is found. We have seen that in the absence of feedbacks, this warming would be 1.2°C. This means that climate feedbacks amplify this warming by a factor of 2 to 4 depending on the model.

Other developments make it possible to use the feedback parameters to estimate the temperature increase due to the Planck response and to the various feedbacks (Dufresne and Bony, 2008). They were applied to twelve CMIP3 (Coupled Models Intercomparison Project) models, and the results are shown in Figure 10.10 illustrating both the average contribution of the models and the inter-model dispersion. These results were confirmed for the CMIP5 models (Vial *et al.*, 2013).

Several of the mechanisms governing the feedback parameter values, and hence the gain, are now well identified (Bony *et al.*, 2006). For example, an increase in the temperature of the atmosphere increases the saturation vapor pressure of the water vapor. If there is little variation in the relative humidity, this results in an increase in the concentration of water vapor in the atmosphere, and therefore in the greenhouse effect, thus constituting a very powerful amplification mechanism of the warming: 1.7°C on average for the models considered here.

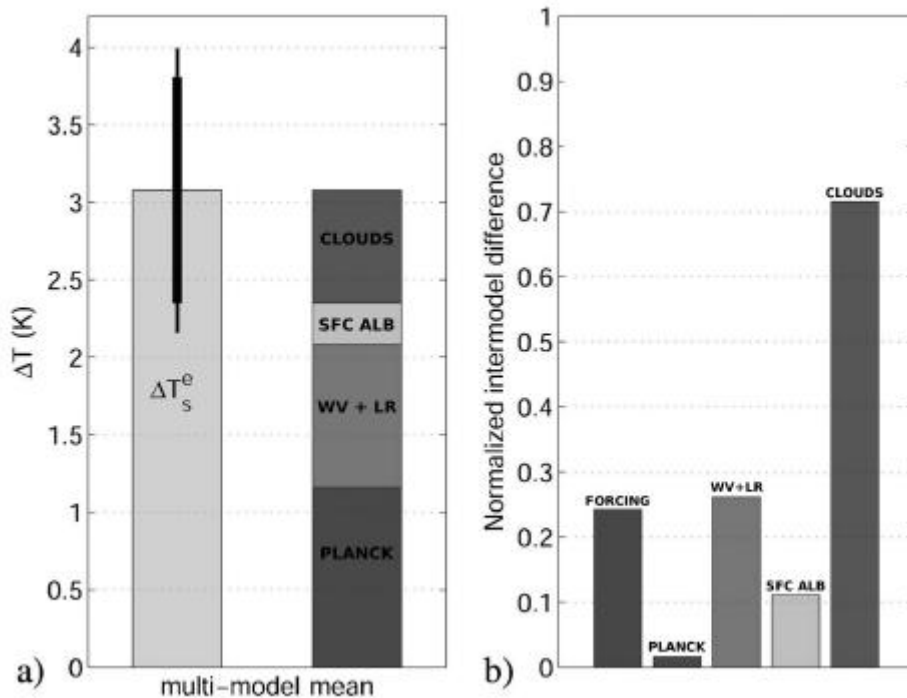


Fig. 10.10: For a doubling of atmospheric CO₂: a) bar on the left, multi-model mean ± 1 standard deviation of increase in global temperature (ΔT_e , °C) and, bar on the right, part of this increase due to the Planck response and to the different feedbacks: combined effects of water vapor and temperature gradient (WV + LR), surface albedo and clouds. b) Standard deviation of the inter-model difference in temperature increase attributable to radiative forcing, the Planck response, and various feedbacks, normalized by the standard deviation of the increase in global temperature. According to Dufresne and Bony (2008).

For thermodynamic reasons (variation of the adiabatic temperature gradient as a function of humidity), it is also expected that, in the case of a humid tropical atmosphere, variations in water vapor will be accompanied by greater warming at high altitudes than close to the surface (except at high latitudes). This increases the emission of infrared radiation from the upper atmosphere and is the only negative feedback: it decreases warming (-0.8°C on average). As these two feedbacks are very strongly correlated for physical reasons, their combined effect is generally considered to contribute about 1°C to the increase in mean temperature (Fig. 10.10a).

The mechanisms behind the surface albedo feedback are also well identified: an increase in temperature increases the melting of snow and ice. This decreases the area covered by surfaces that reflect solar radiation, and therefore increases the amount of energy absorbed by the Earth. This effect contributes about 0.2°C to the temperature increase (Fig. 10.10a).

Finally, the increase in temperature is likely to impact cloud cover. As seen before, clouds exert two opposing effects on the terrestrial radiative balance: on the one hand, by reflecting solar radiation, they contribute to a cooling of the Earth, and on the other, by absorbing infrared radiation, they contribute to increase the greenhouse effect. The relative importance of these two effects depends on multiple factors. The average contribution of clouds estimated by the models considered here is equivalent to a warming of 0.7°C (Fig. 10.10a). However, the dispersion between models is high (Fig. 10.10b): while some models predict a relatively neutral cloud response, most predict a decrease in cloud cover as temperature increases and an increase in global warming of up to 2°C .

Recent studies indicate that this uncertainty stems mainly from the way different climate models predict the response of low clouds (stratus, stratocumulus or small cumulus clouds) to global warming. The way other clouds (including large cumulonimbus storm clouds) respond to climate change is also uncertain. This response contributes only poorly to the uncertainty on the magnitude of global warming, but contributes strongly to uncertainties in regional precipitation changes associated with global warming.

Other feedbacks exist in the climate system, for example, those potentially causing changes in the atmospheric carbon storage capabilities by the ocean and the biosphere. They will be discussed below (Section 10.3.3).

10.3.2 Future scenarios

It is important to keep in mind that the future climate cannot be accurately predicted. This can be explained by several reasons including model uncertainties, uncertainties in scenarios of future greenhouse gas emissions and uncertainties in natural disturbances, such as volcanism, having a strong impact on radiative forcing. However, we can try to answer specific questions: independently of the natural forcings, how would the climate evolve if greenhouse gas emissions followed this or that emission pathway? To this end, various socio-economic scenarios for the evolution of human activities have been established. Four representative concentration pathways (RCP) scenarios have been selected, labeled by a value that corresponds approximatively to the radiative forcing in 2100: RCP2.6, RCP4.5, RCP6.0, RCP8.5 (top of Fig. 10.11). On one extreme, CO_2 emissions rapidly stabilize and then decrease down to zero before 2100 for scenario RCP2.6. On the other extreme, CO_2 emissions continue to grow until 2100 for scenario RCP8.5, which is

for now the most realistic one. CO₂ emissions are mainly due to the use of fossil fuels (oil, coal, gas) and to the SO₂ emissions from the sulfur contained in these fuels. Mainly for health reasons, fuels are increasingly purified of sulfur before use, resulting in a slower increase in CO₂ emissions (or a faster reduction) than for CO₂ in almost all scenarios. For the last IPCC exercise (IPCC, 2013), the concentrations of the different gases were calculated from their emissions by biogeochemical cycle models and by chemical-transport models for sulfate aerosols. The concentrations of each of these constituents can then be used to calculate the corresponding radiative forcing. For example, the evolution of the different forcings from 1860 to 2100 for the RCP8.5 scenarios is shown at the bottom of Fig. 10.11.

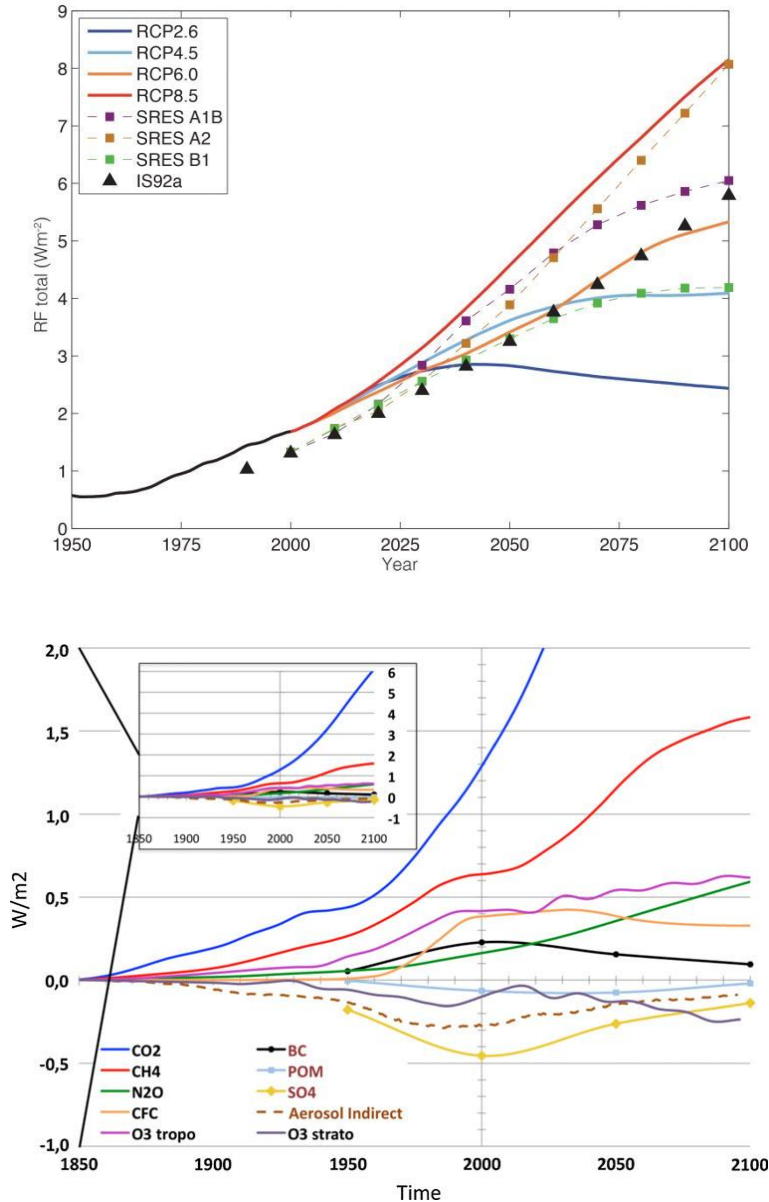


Fig. 10.11: Top: Time evolution of the total radiative forcing (in W/m²) due to human activities for the three SRES emission scenarios used in IPCC-AR4 (IPCC, 2007) and the four RCP scenarios used in IPCC-AR5

(IPCC, 2013). Bottom: Temporal evolution of the radiative forcing (in W/m^2) due to the different chemical agents for the scenario RCP8.5 (Szopa *et al.*, 2013).

10.3.3 The CO₂ cycle

As described in Chapter 2, the carbon cycle is strongly linked to the living world. Understanding the roles of the two main reservoirs, the ocean and the terrestrial biosphere, is therefore crucial to understanding how atmospheric CO₂ will evolve in the coming decades. The ocean is the largest carbon reservoir (holding 40 times the atmospheric content) and can regulate the atmospheric CO₂ concentration by exchanging CO₂ with the atmosphere. These exchanges depend largely on the vertical carbon gradient in the ocean: surface waters are depleted of inorganic carbon and mineral salts; conversely, the deep ocean is enriched in carbon and mineral salts. The existence of this vertical gradient is driven mainly by ocean biology, which establishes a biological pump and transfers carbon from the surface to the bottom. Any modification of this pump may ultimately influence the atmospheric reservoir.

What about anthropogenic disturbances and their impacts on the carbon cycle? These impacts are manifold: a direct chemical consequence of the increase in atmospheric CO₂ is the acidification of the oceans; a thermal consequence of the warming of the water is a decrease in the capacity of the ocean to absorb CO₂, and a biological effect is a modification in the distribution of species due to environmental changes (salinity, temperature) which can cause transformations in the trophic chain and therefore in the biological pump. In terms of CO₂ sinks, it is now known that for two CO₂ molecules emitted, only one remains in the atmospheric reservoir while the other is stored either in the terrestrial biosphere or in the ocean. This ratio is the result of many processes involved in the regulation of the carbon cycle; therefore, due to the anthropogenic perturbation it is expected to vary. The capacity of continents to store carbon can change either gradually or abruptly. For example, permafrost thawing in Siberia would release the equivalent of an additional 100 ppm of CO₂ at least into the atmosphere. As for the biological pump, this will depend on how life functions and adapts in a warming world, which is not easy to predict.

10.4 Climate projections for 2100: What the models say: main climate characteristics

In this section, the results are derived, unless otherwise indicated, from simulations performed by the forty or so coupled atmosphere-ocean general circulation models (or climate models) that contributed to the CMIP5 exercise. The values given below are the average of the models \pm 1 standard deviation.

10.4.1 The amplitude of the warming

In response to both anthropogenic (greenhouse gases and aerosols) and natural (volcanoes and solar intensity) forcings, the models simulate an average global increase in air temperature near the surface of about 0.8°C between the beginning and the end of the 20th century, consistent with observed measurements. Sensitivity studies, with different forcings, have shown that this warming is mainly due to anthropogenic forcings. Today, the climate system is out of balance; if the

concentrations of greenhouse gases and aerosols were maintained at their 2000 values, the climate would continue to warm by around 0.4°C through the 21st century. However, the simulated increase in temperature depends above all on the emission scenarios. Indeed over twenty models, when the concentration of greenhouse gases is prescribed, there is on average a variation of a little less than 1°C for the RCP2.6 scenario and of 4°C for the RCP8.5 scenario (Fig. 10.12). The dispersion of the simulated warming by the different models at the end of the century is $\pm 0.5^\circ\text{C}$, the main reasons for which are outlined in section 10.3.1 of this chapter.

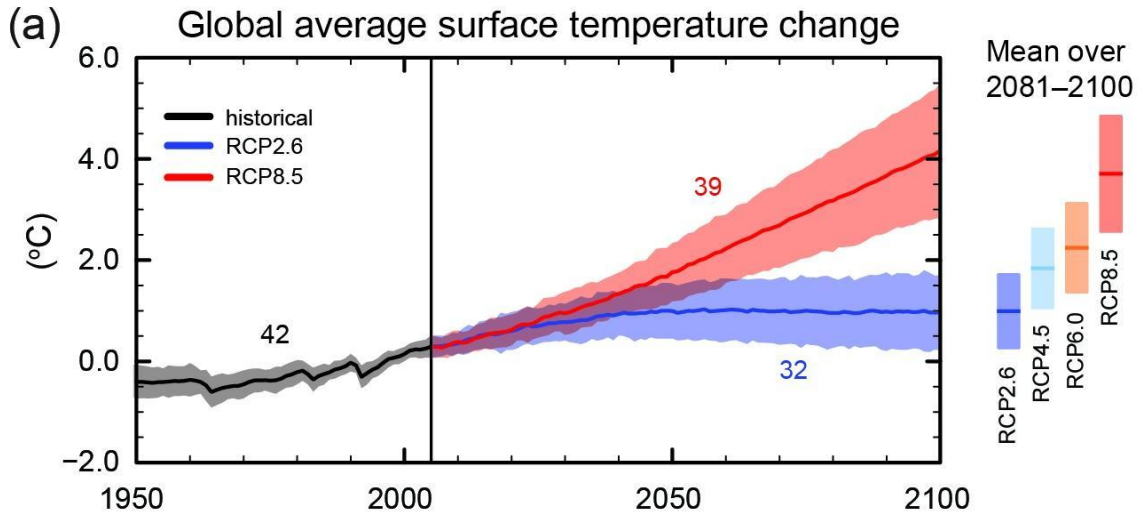


Fig. 10.12: Multi-model time series of air surface temperature anomaly ($^\circ\text{C}$) (compared to the 1986-2005 average), for the 20th and 21st centuries under two different scenarios with very contrasting emission scenarios: RCP2.6 (blue) and RCP8.5 (red). The mean and associated uncertainties averaged over 2081-2100 are given for all RCP scenarios as colored vertical bars. The line represents the average of the models and the light-colored regions, the spread.

10.4.2 Geographical distribution of temperature changes

The geographical distribution of the temperature increase is roughly similar for the different scenarios (although the amplitudes are very different). Figure 10.13 illustrates the RCP2.6 and RCP8.5 scenarios. It shows results that are now well established: the temperature increase is higher on land than on the oceans, and is particularly strong in the high latitudes of the northern hemisphere.

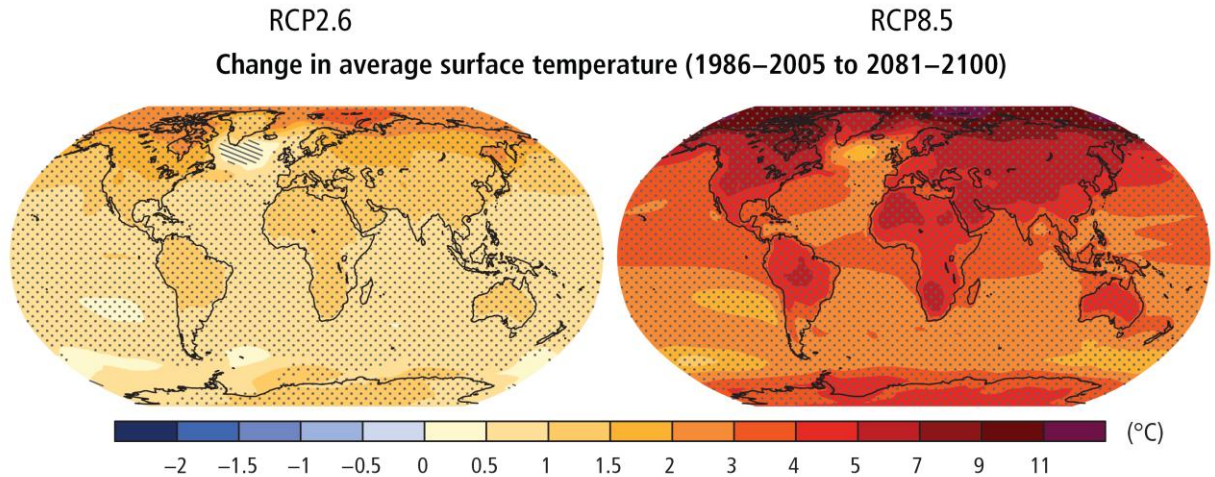


Fig. 10.13: Multi-model average of the difference in air surface temperature (°C), between the end of the 21st century (2081–2100) and the end of the 20th century (1986–2005), for the RCP2.6 (left) and RCP8.5 (right) scenarios (Source: IPCC, 2013).

In the tropics, the greater increase in temperature over land than over ocean is partly explained by changes in evaporation. Over the oceans, the amount of water available for evaporation is not limited, while on the continents it depends on the amount of water available in the soil, and thus, on the amount of precipitation. Due to latent heat exchanges, evaporation cools the surface and this cooling effect is larger over the oceans than over continental areas. For example, with the IPSL model, evaporative cooling is found to reduce the surface radiative balance by 9.8 W/m^2 over the ocean against only 0.2 W/m^2 over the continents. Other processes, such as changing cloud cover or changing atmospheric circulation, also play a role in the ocean-continent warming differential.

In the mid and high latitude regions, the smaller increase in ocean surface temperature is partly due to its thermal inertia. This is particularly true in the southern hemisphere, where very strong winds cause great mixing of the ocean, and where the ocean temperature remains homogeneous to a considerable depth. In order for the temperature of the ocean surface to increase, a large amount of water must be heated up.

The larger increase in temperature in the high latitudes of the northern hemisphere is partly due to the surface albedo feedback. The increase in temperature is accompanied by a decrease in snow cover and sea ice extent in spring and summer. This reduces the reflection of solar radiation at the surface, increases the amount of radiation absorbed and tends to amplify the initial increase in temperature. In regions where the sea ice thins, or even disappears, air temperature rises sharply as the temperature of the ocean surface is higher than that of sea ice. Finally, a change in atmospheric circulation (and in particular the increase in water vapor transported to the high latitudes) is another reason for the strong increase in temperature in these regions. In the south and east of Greenland, it is noted that the temperature of the air near the surface increases only slightly. This trend is more or less marked depending on the model, with some even simulating a slight local cooling. The reason for this is a change in the ocean circulation, and especially in the thermohaline circulation. In these areas, the density of sea water decreases at the surface because of increasing temperatures and/or precipitation. Surface waters are no longer dense enough to sink, reducing oceanic convection and the associated North Atlantic drift. The effect of this density reduction on temperature depends on the model, both in terms of amplitude and geographical

extension. It modulates global warming locally and influences global warming slightly, but nevertheless this warming remains significant on all continents of the northern hemisphere, especially in Europe.

10.4.3 Changes in precipitation

Although there is a large spread between climate models, on average, they project an increase in precipitation over the 21st century alongside increased temperatures (IPCC, 2013). Projected precipitation changes exceed 0.05 mm/day and 0.15 mm/day with the RCP2.6 and RCP8.5 scenarios respectively. These changes are far from being spatially homogeneous and exhibit a strong seasonal variability (Fig. 10.14). However, if we consider the zonal means, there is a tendency towards increased precipitation everywhere, except in the subtropical regions (around 30°N and 30°S) and in the Mediterranean basin where they decrease. The general increase in precipitation is due to the increase in atmospheric water vapor content, while the decrease simulated in the subtropical regions is related to a change in atmospheric circulation.

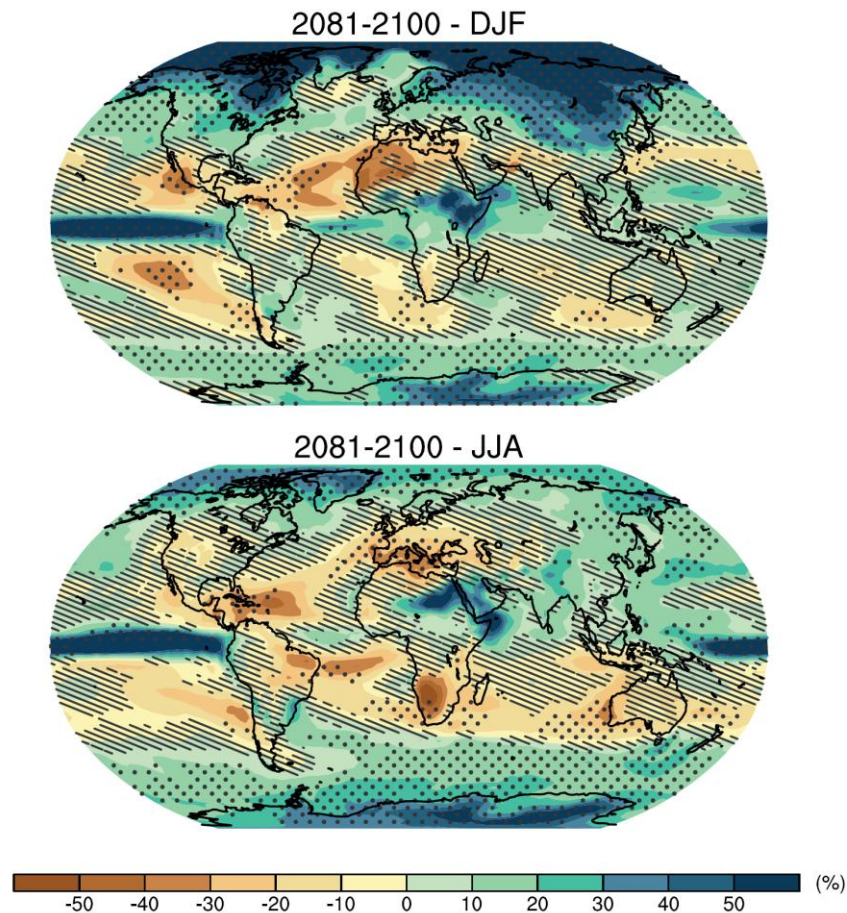


Fig. 10.14: Multi-model average of the precipitation difference (%) between the end of the 21st century (average between 2081 to 2100) and the end of the 20th century (average between 1980 to 1999), for the RCP8.5 scenario for December-January-February (*top*) and (*bottom*) June-July-August. Hatching indicates regions where the multi-model mean change is less than one standard deviation of internal variability.

Stippling indicates regions where the multi-model mean change is greater than two standard deviations of internal variability and where at least 90% of models agree on the sign of change.

It can be seen that the models consistently simulate a year-round increase in precipitation at high latitudes, and a winter increase in the mid-latitudes (Fig. 10.14). Similarly, they consistently simulate a decrease in precipitation in subtropical regions. In Europe, models simulate an increase in precipitation in the north and, on the contrary, a drying up around the Mediterranean Basin. On the other hand, changes in precipitation in the equatorial and tropical regions are not consistent from one model to the other, especially on the continents such as South America, West and Central Africa, India and South-East Asia. In these areas, some models simulate a decrease in precipitation, while others simulate an increase. These differences between models are particularly pronounced in the monsoon regions. In general, changes in precipitation on the continents remain very uncertain, even in terms of annual mean. This is due to major uncertainties in the representation of the different processes. Currently, there is no clear way of identifying which of the results are the most reliable.

10.4.4 Changes in storm patterns

Under climate change, the characteristics of lows in the mid-latitudes (particularly those reaching the coast of Brittany) are likely to change for two reasons: the first is a change in the equator-pole temperature gradient, which tends to decrease near the surface but to increase with altitude. The second reason is an increase in the total amount of water vapor in the atmosphere, and in turn, in the amount of water vapor that can be condensed and thus release latent heat. In climate change simulations, we observe a poleward shift of low-pressure, a reduction in the total number of depressions, but an increase in the number of deeper and hence stronger troughs. For example, according to the diagnoses made by Lambert and Fyfe (2006), the models simulate, on average, in 2100 and for a moderate greenhouse gas scenario, a decrease in the total number of depressions of around 10% in the southern hemisphere and a little less in the northern hemisphere. They also simulate an increase of 20% of the number of intense depressions in the northern hemisphere and of 40% in the southern hemisphere.

10.4.5 Evolution of sea ice

The analysis of CMIP3 and CMIP5 models clearly highlights a sea-ice decline in the course of the 21st century, the dominant factor being the rising summer temperatures rather than the winter ones which are projected to remain negative. Though most of the CMIP5 models project a nearly ice-free Arctic Ocean by 2100 with a sea ice extent of less than 1×10^6 km² (for at least 5 consecutive years) at the end of summer in the RCP8.5 scenario, some show large changes occurring before 2050. However, these results are strongly dependent on the ability of models to reproduce the climatological mean state of the Arctic sea ice cover over 1979-2012. Based on the CMIP5 multi-model ensemble, projections of average reductions in Arctic sea ice extent for 2081–2100 compared to 1986–2005 range from 8% (RCP2.6) to 34% (RCP8.5) in February and from 43% (RCP2.6) to 94% (RCP8.5) in September. The evolution of sea ice around the Antarctic is more uncertain. The CMIP5 multi-model mean projects a decrease in sea ice extent ranging from 16% for RCP2.6 to 67% for RCP8.5 in February and from 8% for RCP2.6 to 30% for RCP8.5 in September for 2081–2100 compared to 1986–2005. There is, however, low confidence in those values because of the wide inter-model spread and the inability of almost all of the available

models to reproduce the mean annual cycle, the interannual variability and the overall increase of the Antarctic sea ice coverage observed during the satellite era.

10.4.6 Evolution of continental ice

Retreat of the glaciers

Glaciers react quickly to climatic effects and are thus good indicators of climate change. For more than a century, and especially since the 1980s, the retreat of glaciers has been a phenomenon occurring almost everywhere on the globe. This phenomenon is likely to increase in the 21st century with the rising temperatures, and could even lead to the disappearance of certain glaciers in the coming decades. Projections of the future evolution of glaciers depend, on the one hand, on climate scenarios but also, on their sensitivity to global warming.

Glaciers located in dry and cold regions (such as the Canadian Arctic) have low sensitivity to global warming and are more prone to resist. On the contrary, glaciers located in coastal regions are subject to oceanic influence and have a greater sensitivity to global warming. This is the case for Norwegian glaciers, for example. In recent decades, these have tended to grow due to increased precipitation. But in recent years, this trend seems to have been reversed. Alpine glaciers are in an intermediate situation. We will not review exhaustively the melting of glaciers, but we chose to illustrate this behavior through the study of two alpine glaciers.

At the Environment Geosciences Institute of Grenoble (IGE), two studies were carried out on alpine glaciers, one on the Saint-Sorlin, the other at the dome of Goûter, in the Mont-Blanc massif.

The first study simulated the future evolution of the mass balance of the Saint-Sorlin, located in the Grandes Rousses massif whose highest point is at 3,400 meters altitude. The results show that even with an optimistic greenhouse gas emission scenario (+1.8°C in 2100), the equilibrium line (i.e. the lowest limit of eternal snow) is at a higher altitude than the highest point of the glacier. This means that over a full year, the glacier does not accumulate snow (or ice) and is therefore, in a state of chronic ablation. In order to simulate the dynamic response of the glacier, these results were then used as inputs to a two-dimensional ice flow model. Despite a moderate global warming, the model suggests a complete disappearance of the glacier around 2070. The dynamic response of the glaciers is complex because it depends not only on their specific morphology, which is different from one glacier to another, but also on many physical processes which are sometimes difficult to simulate and which determine their temporal response, i.e. on what timescale the glacier will grow or, on the contrary, disappear. Nevertheless, this study suggests that alpine glaciers similar in size and located at an altitude close to that of the Saint-Sorlin, could undergo the same type of evolution in the 21st century under the influence of moderate global warming.

The second study is based on borehole temperature measurements (140 m deep) located at the Dome du Goûter at 4,250 m altitude. These measurements showed a warming of 1 to 1.5°C over the first 60 meters of ice, between 1994 and 2005. A physical modeling of the process of heat diffusion in the ice made it possible to show that the observed warming in results not only from atmospheric warming, but also from the heat produced by the refreezing of surface melt water that percolates at depth.

Moreover, simulations carried out for different global warming scenarios confirm the 21st century trend and show that, regardless of the global warming scenario, the Alpine glaciers, currently classified as 'cold' and located between 3,500 and 4,250 m altitude with an internal temperature ranging from 0 to -11°C, could become 'temperate', with an internal temperature close to melting point.

Other modeling studies using different greenhouse gas scenarios lead to similar and equally disturbing conclusions. A study conducted in the Montana region in the Glacier National Park shows that, with a doubling of CO₂, some glaciers would disappear by 2030, despite an increase of 5 to 10% in average precipitation in the mid and high latitudes.

The future of ice sheets

There are different approaches to determine how polar ice sheets will evolve in the future. The first is to determine the surface mass balance of the ice sheets which is directly dependent on the climate. To simulate as precisely as possible the mass balance of the ice sheets, high-resolution climate models are necessary to properly represent the topography of the ice sheets, especially the steep slopes at the margins. These areas correspond to the ablation zones and are also the locations where most of the precipitation falls. However, AOGCMs usually tend to overestimate precipitation and underestimate ablation. In addition, snowpack models implemented in general circulation models are often too simplistic and do not account for key processes taking place in the snowpack. Among the missing processes are the refreezing of surface melt water that percolates at depth, the transport of snow by winds, the snow metamorphism and the transformation of snow into ice. These processes are crucial for the estimates of surface mass balance. For example, water refreezing modulates surface runoff and snow metamorphism strongly modifies the albedo and thus the surface energy balance.

Regional atmospheric models generally offer a better representation of the surface energy balance scheme than AOGCMs because of their finer resolution and the inclusion of more sophisticated snow models. However, as they are forced at their lateral boundaries by outputs from global climate models, they may suffer from the global model deficiencies. As a result, the uncertainties associated with the GCM-based forcing represent about half of the uncertainty associated with SMB changes inferred from regional climate models (RCM). All RCM-based studies project an increase in precipitation over large parts of Greenland and Antarctic ice sheets in response to global warming, but there is great uncertainty as to the magnitude of this increase. Projections suggest that over Greenland, ablation will largely exceed the increase in rainfall. Conversely, in East Antarctica, precipitation is expected to exceed ablation throughout the 21st century, but the key question is whether the mass gain will be offset by dynamical ice losses from the West Antarctic ice sheet.

The surface mass balance is not the only important parameter in the determination of the evolution of polar ice sheets. As explained earlier, their dynamic response must also be considered. This can be achieved through the use of three-dimensional ice-sheet models which include most of the processes responsible for the ice-sheet evolution as a function of climate forcing (temperatures and precipitation or surface mass balance). For a more thorough description of ice-sheet models, we ask the reader to refer to Chapter 3 of this volume. However, several problems may arise when using such models. As previously mentioned, the surface mass balance can be

computed by a climate model (RCM or AOGCM), but frequently, ablation is still determined from an empirical formulation that relates the number of positive-degree-days (integral of positive temperatures) to the snow and ice melting rates. The main drawback of this approach is that it does not account for albedo changes. Moreover, it has been validated on only a few Greenland sites for the present-day period. The mass balance derived from such methods is generally more uncertain than that obtained using regional models. Another difficulty is linked to the difference of resolution between climate and ice-sheet models. As temperature, precipitation and surface mass balance are highly dependent on topography. This requires the development of appropriate techniques to account for the effect of altitude.

In addition, researchers still face many challenges in representing some processes related to rapid dynamics, such as those occurring at the base of the ice sheet or at the ice-ocean interface, where small disturbances seem capable of triggering strong instabilities, which can propagate up to a thousand kilometers upstream, and lead to a destabilization of the entire ice sheet. However, understanding the impact of small-scale processes on the large scale is still in its infancy. Over the last two decades, observations have shown an increase in the flow of outlet glaciers, suggesting that these could respond much more quickly than previously expected to variations in atmospheric and oceanic conditions, making possible a significant retreat of the ice sheet in the more or less distant future. The physical laws governing ice flow in these glaciers still remain poorly known. For example, although the marine ice-sheet instability is increasingly well represented in new generation ice-sheet models, there is no consensus on hydro-fracturing yet. Large uncertainties also exist on the physical laws governing iceberg calving and basal melting under the ice shelves. A last, but not least, problem is related to the initial state of the ice sheets. Indeed, starting future short-term (a few centuries) simulations from a realistic present-day state of the ice sheet is of primary importance to avoid as much as possible spurious biases in the results. Getting an accurate initial state is challenging however because of the scarcity of observations on vertical velocity and temperature profiles, on basal conditions (e.g. frozen or thawed bed areas, bedrock topography). Several approaches have been developed ranging from long free evolving simulations over one or several glacial and interglacial cycles to more formal optimization approaches often based on inversion techniques, with various target criteria (either surface velocities or topography in agreement with observations, or internal properties accounting for the past history of ice sheets). Each of these techniques presents some advantages and drawbacks, but their efficiency should improve in the future as the number of observations grows. Recent remote sensing observations made over Greenland and Antarctica are expected to refine numerical simulations and thus to improve the relevance of future forecasting models. Finally, part of the uncertainty in the future ice-sheet responses comes from uncertainty in the climate forcing itself. This is due to our lack of knowledge in the future socio-economic pathways and the biases in the climate models. Moreover, climate-ice sheet interactions are still very rarely taken into account in the models. Accounting for these interactions may have the potential to strongly modify not only the simulated climate and ice-sheet responses but also sea-level projections (Bronse laer *et al.*, 2018; Golle dge *et al.*, 2019).

10.4.7 Sea level change

We have seen, in the first part of this chapter, that at the scale of a few decades, the main causes of sea-level variations are due, on the one hand, to the thermal expansion of the ocean (in the case of a warming climate), and on the other hand, to changes in the mass of water in the ocean due to exchanges with continental reservoirs. Based on the results from 21 AOGCMs, the sea-level

projections reported in the fifth IPCC report (IPCC, 2013), all show an increase in sea-level by the end of the 21st century (2081-2100) compared to the 1986-2005 period, with an average global mean sea-level rise ranging from 0.28 to 0.61 m for RCP2.6 and from 0.52 to 0.98 m for RCP8.5. For the RCP8.5 scenario, the rate of sea-level rise increases throughout the 21st century, going from 3.2 ± 0.4 mm/yr (for the 1993-2010 period) to 11.2 mm/yr (2081-2100), whereas, in the RCP2.6 scenario, the rate increases up to 4.4 mm/yr around 2050 and slightly declines in the second half of the century.

According to the IPCC report (IPCC, 2013), thermal expansion remains the main contributor (30 to 55 %) to global mean sea-level rise over the 21st century with median rates of 0.14 ± 0.04 m (RCP2.6) and 0.27 ± 0.04 m (RCP8.5) in 2081-2100. These contributions can be estimated from changes in ocean heat uptake increasing roughly linearly with global mean surface air temperatures simulated by the AOGCMs. It should be noted that AOGCM simulations do not include volcanic forcing which may reduce the projected contribution of thermal expansion.

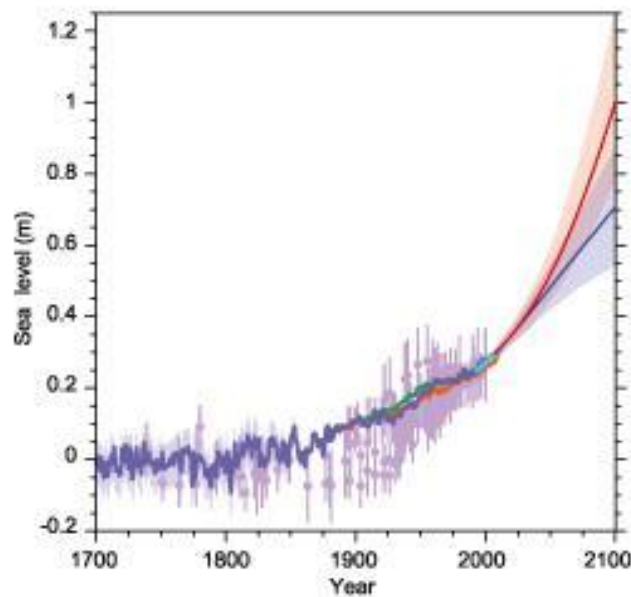


Fig 10.15: Compilation of paleo sea level data, tide gauge data, altimeter data and central estimates and likely ranges for projections of global mean sea level rise for RCP2.6 (blue) and RCP8.5 (red) scenarios, all relative to pre-industrial values (Source: IPCC, 2013).

The AOGCM simulations forced by the different RCP scenarios highlight a spatial variability of the sea level (Fig. 10.16). As they do not take into account the freshwater fluxes coming from ice sheets, this regional variability, previously observed in satellite measurements over the 1993-2010 period, is linked to a variability in the atmosphere-ocean-sea-ice system. More specifically, regional variability can be due not only to variations in temperature and salinity (i.e. precipitation/evaporation ratio) and therefore density, but also to variations in ocean and atmospheric circulations (variations in wind direction and intensity). From one model to another, the spatial distributions of sea level variations are not identical. However, some common features emerge in the projections for the end of the 21st century that are identified in Figure 10.16. For example, the Southern Ocean is characterized by a lower-than-average sea level rise, likely related

to changes in wind stress and heat fluxes, which are also responsible for the greater sea-level rise in the Pacific (Bouttes and Gregory, 2014). A dipole pattern with greater sea-level rise to the north and smaller sea-level rise in the south can also be seen in the North Atlantic and is attributed to changes in heat and freshwater fluxes.

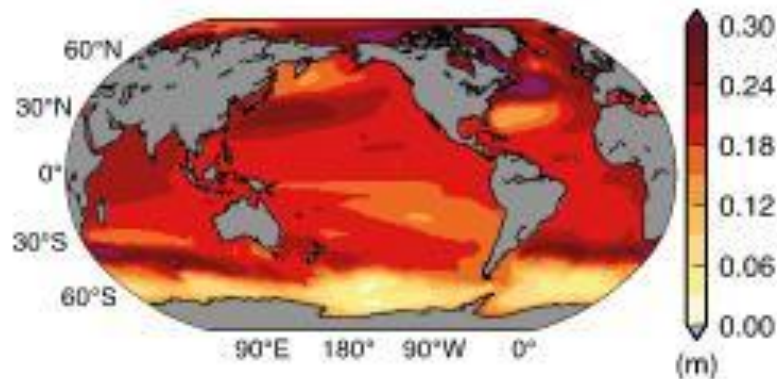


Fig. 10.16: Ensemble mean projection of the time-averaged dynamic and steric sea-level changes for the period 2081–2100 relative to the reference period 1986–2005, computed from 21 CMIP5 climate models (in meters), using the RCP4.5 experiment. The figure includes the globally-averaged steric sea level increase of 0.18 ± 0.05 m (Source: IPCC, 2013).

While changes in sea level due to thermal expansion can easily be determined from climate models, we have seen in the previous section that there are significant uncertainties in the simulation of future continental ice. These uncertainties dominate the projections of sea-level rise resulting from the ice-sheet surface melting, dynamic ice discharges or iceberg calving. As a result, these projections are not very different from one climate scenario to another. For example, in the last IPCC report (IPCC, 2013), the contribution from the ice-sheet rapid dynamics is estimated to be between 0.03 and 0.19 m for the RCP2.6 scenario and between 0.03 and 0.20 m for the RCP8.5 scenario.

To better represent the contribution of polar ice sheets to sea-level rise in the future, an accurate representation of rapid ice dynamics in ice-sheet models is of primary importance. The resolution (5–10 km) of the previous generation of three-dimensional large-scale ice-sheet models is not fine enough to properly capture the rapid ice streams whose characteristic spatial scale may be smaller than 1 km in some cases. Moreover, these models are based on approximations resulting in simplified equations of ice dynamics. While these approximations are crucial to investigate the ice-sheet behavior at the multi-millennial time scale, they may cause deficiencies in the representation of rapid ice dynamics as well as in the representation of grounding line migration, which plays a crucial role in ice-sheet evolution as mentioned earlier. However, significant progress has been made in the development of ice-sheet models, such as the Full Stokes models (e.g. Gillet-Chaulet *et al.*, 2012). These models do not rely on simplifying assumptions and have an adaptive mesh that may be less than 1 km at the ice-sheet margins, thereby providing a more accurate representation of ice-sheet dynamics. However, these models are highly expensive in terms of computational time and have not yet been applied to the whole Antarctic ice sheet. A second limiting factor is related to the fact that some processes remain poorly constrained due to the scarcity of observations (e.g. basal conditions or hydro-fracturing), or poorly understood (e.g.

basal melting under the ice shelves or iceberg calving). Finally, as mentioned in the previous section, there is a crucial need to develop Earth System Models which account for the feedbacks between climate and ice sheets so as to refine sea-level projections.

It is important to note that since the last IPCC report was published (IPCC, 2013), many projections coming from individual studies have provided higher estimates of the projected sea-level rise compared to those reported by the IPCC (0.52 to 0.98 m for the highest emission scenario). The main reasons for this disagreement are related to the large uncertainties associated with the future ice-sheet evolution and to the fact that the IPCC only selected the most likely range of sea-level rise estimates and excluded the more extreme (considered as less likely) outcomes. All the projections together give a range of 0.16 – 2.54 m in 2100 (Garner *et al.*, 2019) which reflects the large uncertainties in the maximum contribution of Greenland and Antarctica (DeConto and Pollard, 2016) and suggests the possibility for these ice sheets to become the main contributor to global mean sea-level rise in the course of the 21st century.

10.5 The climate of the next millennium: towards integrated modeling of the Earth system

10.5.1 Climate change: anthropogenic disturbance versus variations in insolation

In Chapter 7, we analyzed in detail the climate variations induced by the orbital parameter variations over the scale of tens of thousands of years. We are interested here in much longer time scales ranging from 100,000 to millions of years. The amplitude of warming projected by climate models over the next decades and even the next century raises questions about the impact of this profound change in the climate system over several millennia, especially as the acceleration of CO₂ emissions suggests that the magnitude of the perturbation may be even greater than that predicted by the most pessimistic scenario.

Data from Vostok and EPICA ice cores in Antarctica, showed that atmospheric CO₂ varied by about 100 ppm during the transition from an ice age to an interglacial period, and that these variations were correlated with changes in air temperatures, suggesting a link between CO₂ and climate. Today, this link is commonly accepted and attention is focused on global warming due to the increase in greenhouse gases in the atmosphere. However almost forty years ago, in 1972, the climatological community met in the United States to discuss the imminence of the next ice age. This question arose because geological data showed that for about a million years, the Earth had alternated between cold episodes corresponding to the glaciation phases, and the warmer interglacial periods, with a pseudo-periodicity of 100,000 years.

Data available in 1972 showed that the previous two interglacial periods had lasted about 10,000 years. Yet, the Holocene, the interglacial period we are currently experiencing, has been going on for 10,000 years. It seemed therefore reasonable to think that this warm phase would soon end and give way to a new ice age. This reasoning was based on the assumption that all interglacial periods are of equal duration. However, although the first numerical experiments carried out with statistical models indicated that the cooling initiated 6,000 years ago (after the

Holocene climate optimum) would continue in the future, Oerlemans and Van der Veen (1984) of the University of Utrecht showed, with an ice-sheet model, that the transition to a new glacial phase would not occur before 50 000 years.

Based on data from marine sediments and ice cores, it is now well established that the duration of an interglacial period varies considerably from one cycle to the next. The same models used to predict the future were used to simulate the last interglacial-glacial transition. Indeed, taking into account the atmosphere-ocean feedbacks, these models produce perennial snow in the Canadian archipelago (Khodri *et al.*, 2001). It is also known that the Earth's orbital parameters (see Chapter 7) that govern the seasonal and latitudinal distribution of solar energy can vary considerably from one cycle to another. For example, geological data tell us that the interglacial period occurring 400,000 years ago (marine isotopic stage 11) was exceptionally long. This situation corresponds to a weak eccentricity where the seasonal and latitudinal distribution of solar energy varied very little. Celestial mechanics tell us that a similar situation should recur within 20,000 years, and for this reason the marine isotopic stage 11 is often considered to be one of the best analogues for the future climate. Many internal feedbacks generated by the different components of the climate system amplify or reduce the effect of the latitudinal and seasonal distribution of insolation. Thus, climate projections on the scale of a few hundreds of thousands of years require the variations of both insolation and atmospheric CO₂ (and other greenhouse gases) to be taken into account in models including representations of the atmosphere, ocean, cryosphere, lithosphere and vegetation.

One of the first models of this type was developed for the Northern hemisphere at the University of Louvain-la-Neuve, Belgium (Gallée *et al.*, 1992). It successfully reproduced the main characteristics of the current climate, as well as the variations in ice volume during glacial-interglacial cycles. Since the model has been shown to provide reasonable simulations of the 100,000-year cycle, it has been applied as a second step to the simulation of future climates. Several tests have thus been carried out on the climate of the next 130,000 years, either by keeping the CO₂ constant at different levels (290 ppm, 200 ppm and 250 ppm), or by using the CO₂ variations of the last glacial-interglacial cycle (Loutre and Berger, 2000). The results of these simulations suggest, on the one hand, that the climate of the next 50,000 years is particularly sensitive to the level of atmospheric CO₂ concentration and that our current interglacial period will be much longer than any other one in the past. It could last more than 55,000 years with CO₂ levels between 230 and 290 ppm: the first glacial stage would appear around 60,000 AD, and the next glacial maximum (in terms of ice volume) would be around 100,000 AD, followed by a deglaciation phase that would end around 120,000 AD. These results suggest that the marked differences between our interglacial period (present and future) and the previous Quaternary warm periods are due to the small insolation variations that characterize the former. Based on another scenario designed to reproduce the natural variations of CO₂ and not the anthropogenic contribution, other simulations have been carried out, either with a more elaborate version of the Loutre and Berger's model, or with a climate model of intermediate complexity coupled with a more sophisticated model of the evolution of polar ice sheets (Ganopolski *et al.*, 2016). The results of these simulations are in agreement with those presented previously, and show that the next glacial inception will be postponed by at least 100 000 years.

Although, the variations in summer insolation at 65°N have long been considered as the pacemaker of glacial-interglacial transitions, the above results show that, the level of atmospheric

CO₂ will be a key parameter in the future. While the natural variations of CO₂ along with the insolation forcing exclude the possibility of a glacial episode in the future for at least 50,000 years, it is possible that the impact of the anthropogenic contribution will lead to a complete disappearance of polar ice sheets, and that a return to a glacial phase could occur only in 100,000 years. Coupled climate-ice sheet models, validated on the last glacial-interglacial cycle, will make it possible to explore the threshold values of CO₂ which could have long-term effects on the fate of ice sheets.

10.5.2 The long-term future of the polar ice sheets: impact and irreversibility

As seen earlier, the response times of the different components of the climate system are extremely variable, ranging from a few minutes to a few days for the atmosphere and from a few months to several hundreds of years for the ocean. While the ice sheets have long been considered as a slow component of the Earth system (with characteristic time scales ranging from thousands to hundreds of thousands of years), recent observations provide evidences that they can react to climate change far more quickly than previously thought. The last glacial-interglacial cycle demonstrates how deeply the climate is influenced by the slow development and rapid collapse of the ice sheets.

The ice core records retrieved from the Vostok and Dome C sites in Antarctica show that, for 800 000 years, the world has alternated between four ice sheets (during glacial periods) and only two ice sheets (during interglacial periods). In other words, Greenland and Antarctica withstood the warming that led to the disappearance of the Fennoscandian and North American ice sheets. There is no doubt that Greenland and West Antarctica have not always emerged unscathed from glacial-interglacial cycles. Indeed, during the last interglacial period (i.e. 130 – 115 ka ago), the sea level was 6 to 9 m higher (Kopp *et al.*, 2009). It is therefore possible that anthropogenic activity could lead to the partial or total melting of Greenland (Charbit *et al.*, 2008).

Recent observations of Greenland, and, more surprisingly, of Antarctica mass balances (Velicogna, 2009) show that these ice sheets have become one of the main contributors to the increase in sea level (Cazenave *et al.*, 2009). Their complete disappearance would lead to a sea-level rise of nearly 60 m: 6.6 m for Greenland and 52.8 m for Antarctica, of which 3.3 m would come from West Antarctica. These figures should be compared to the 120 m sea-level rise corresponding to the disappearance of the North American and Fennoscandian ice sheets in response to very small changes in insolation compared to the additional radiative forcing from anthropogenic activities. Also, the disappearance of past ice sheets was spread over 14,000 years (from the Last Glacial Maximum to the Mid-Holocene). The long-term effects (several hundred years) of anthropogenic forcing on ice sheets are not easy to model, partly because of uncertainties in the future socio-economic pathways over the 21st century and therefore in the evolution of the greenhouse gas concentrations in the atmosphere. It is therefore even more difficult to establish scenarios over several centuries (Charbit *et al.*, 2008). However, several assumptions can be made about the long-term evolution of greenhouse gas emissions to explore the sensitivity of the present-day ice sheet with numerous scenarios. Performing simulations over several centuries or several millennia cannot be achieved through the use of general circulation models, which are too expensive in terms of computational time, and simplified climate models coupled with efficient ice-sheet models are required.

In fact, there are three different time frames relevant in the study of the evolution of ice sheets. The evolution over the twenty-first century, the basis of all IPCC analyzes, will very likely bring about a rise in sea level of several tens of centimeters (or even more), although there is a great deal of uncertainty linked to the emission scenarios, to climate model biases and to difficulties of ice-sheet models to capture the processes causing rapid dynamical change. The second horizon, beyond the 21st and the following centuries, is one where the CO₂ level may stabilize at three or four times that of the pre-industrial level, likely resulting in a massive retreat of Greenland and West Antarctica. These changes are also likely to modify the ocean circulation and the global climate. If this high level of CO₂ persists for a long time in the atmosphere, the ice-sheet melting could be irreversible, in the sense that there would no longer be any perennial snow in Greenland (Charbit *et al.*, 2008). Finally, there is the much more distant third horizon, which raises the following question: for the last million years, our climate has oscillated between ice ages (long periods of about 100,000 years) and interglacial periods (short periods of about 10,000 years). Is it possible that the anthropogenic perturbation might cause a switch to another climate mode with strongly reduced ice sheets or even no ice sheet at all, similar to the hot climate mode of the pre-Quaternary era? In other words, is it possible that anthropogenic disturbance could induce modifications such that the next marked decline in summer insolation due in about 100,000 years (Loutre and Berger, 2000) might not bring about an ice age?

Even if this question seems ‘futuristic’, we have good reasons to believe that the glacial-interglacial cycles of the last million years will no longer occur because the expected decline of insolation will not be large enough to compensate for the radiative forcing due to the high atmospheric CO₂ levels. This is what is suggested by the results of simulations carried out for periods such as the Pliocene around 3 Ma where the CO₂ level is estimated to have been around 405 ± 50 ppm.

In these scenarios, a key factor is the long time required to reach atmospheric CO₂ equilibrium which can be several tens to hundreds of thousands years (Archer, 1997). The anthropogenic disturbance is almost instantaneous, but its consequences will last for a very long time, and the Milankovitch cycles that have so far allowed glacial-interglacial transitions from through profoundly non-linear processes, can become inoperative in the future. Is it a bit presumptuous though to think that a couple of hundred years of ‘energy profligacy’ leading to a very large increase in atmospheric CO₂ could still be felt tens of thousands of years later? Maybe, but still, it is important to remind that studies of the Earth past climates show that the presence of ice sheets is associated with low CO₂ levels. . It is therefore logical to think that, in a world that sustains high CO₂ concentrations, the behavior of present-day ice sheets will change in the short and medium term.

The world at the beginning of the Cenozoic (with 1,120 ppm of CO₂ in the atmosphere) was much hotter than today. Antarctica was already in its polar position since the end of the Cretaceous (70 Ma ago), but far from forming an ice sheet, it was covered with forests. There was no sign of an ice sheet, until the CO₂ level dropped sufficiently to trigger the progressive freeze-up of Antarctica (DeConto and Pollard, 2003). A planet with no ice sheet is not a figment of the imagination, rather their presence being the exception when viewed over geological times.

This book shows how the face of our planet changed over these time scales: from plate tectonics (millions of years) to the development of huge ice sheets at temperate latitudes (hundreds of thousands of years), with very strong variability in glacial climates at the scale of a few thousand

years. Our own interglacial period, the Holocene, has been much more stable in terms of climate and has contributed to the extraordinary expansion of the human population. With an Earth inhabited by more than 9 billion men and women, it will be essential to manage climate change, in order to protect societies and their environment. The past teaches us that our little blue planet has undergone many changes. It is not the planet that is in danger, it is rather the populations, especially as they do not have an equal standing in the face of climate change. And so, paradoxically, if man has become a major actor in climate change through industrial development and massive use of fossil fuels, he could also suffer at his own expense from upheavals and difficult situations that he himself has created.

References

- Adler, R. F., et al., (2003)**, The Version 2 Global Precipitation Climatology Project (GPCP) Monthly Precipitation Analysis (1979–Present), *Journal of Hydrometeorology*, 4, 1147–1167.
- Allen, R. J. and Sherwood, S. C., (2008)**, Warming Maximum in the Tropical Upper Troposphere Deduced from Thermal Winds, *Nature Geoscience*, 1, 399-403.
- Archer, D., et al., (1997)**, Multiple timescales for neutralization of fossil fuel CO₂, *Geophysical Research Letters*, 24, 405– 408.
- Archer, D., et al., (2009)**, Atmospheric lifetime of fossil fuel carbon dioxide, *Annual Review of Earth and Planetary Sciences*, 37, 117-134, doi: 10.1146/annurevearth031208.100296.
- Bony, S. et al., (2006)**, How Well do we Understand and Evaluate Climate Change Feedback Processes ?, *Journal of Climate*, 19(15), 3 445-3 482.
- Bouttes, N. and Gregory J. M., (2014)**, Attribution of the spatial pattern of CO₂-forced sea level change to ocean surface flux changes, *Environmental Research Letters*, 9, 034004, doi: 10.1088/1748-9326/9/3/034004.
- Bronselaer, B. et al., (2018)**, Change in future climate due to Antarctic meltwater, *Nature*, 564, 53-58, doi: 10.1038/s41586-018-0712-z
- Cazenave, A. et al., (2009)**, Sea Level Budget over 2003-2008: A Reevaluation from GRACE Space Gravimetry; Satellite Altimetry and Argo, *Global and Planetary Change*, 65, 83-88.
- Charbit, S. et al., (2008)**, Amount of CO₂ Emissions Irreversibly Leading to the Total Melting of Greenland, *Geophysical Research Letters*, 35, L12503, doi: 10.1029/2008GLO33472.
- Church, J. A. and White N. J., (2011)**, Sea-level rise from the late 19th to the early 21st century, *Survey of Geophysics*, 32, 585–602.
- Christiansen, H. H., et al., (2010)**, The thermal state of permafrost in the Nordic area during the International Polar Year 2007–2009, *Permafrost Periglacial Processes*, 21, 156–181.

- Clark, P. U., et al., (2016)**, Consequences of twenty-first-century policy for multi-millennial climate and sea-level change, *Nature Climate Change*, 6, 360-369.
- DeConto, R. M. and Pollard, D., (2003)**, Rapid Cenozoic Glaciation of Antarctica Induced by Declining Atmospheric CO₂, *Nature*, 421, 245-249, doi:10.1038/nature01290.
- DeConto, R. M. and Pollard, D., (2016)**, Contribution of Antarctica to past and future sea-level rise, *Nature*, 531, 591-597, doi: 10.1038/nature17145.
- Defrance, D., et al., (2017)**, Consequences of rapid ice-sheet melting on the Sahelian population vulnerability, *Proceedings of the National Academy of Sciences*, 114 (25) doi: 10.1073/pnas.1619358114.
- Dufresne, J.-L. and Bony, S., (2008)**, An Assessment of the Primary Sources of Spread of Global Warming Estimates from Coupled Atmosphere-Ocean Models, *Journal of Climate*, 21(19), 5 135-5 144, doi: 10.1175/2008JCLI2239.1.
- Dufresne J-L and Saint-Lu M., (2016)**. Positive feedback in climate: stabilization or runaway, illustrated by a simple experiment *Bulletin of American Meteorological Society*, 97(5), 755-765, doi: 10.1175/BAMS-D-14-00022.1
- Fourier J.-B. (1824)**, Remarques générales sur les températures du globe terrestre et des espaces planétaires. *Annales de Chimie et de Physique*, 2e série, XXVII, 136-167
- Gallée, H. et al., (1992)**, Simulation of the Last Glacial Cycle by a Coupled, Sectorially Averaged Climate-Ice-Sheet Model 2. Response to Insolation and CO₂ Variations, *Journal of Geophysical Research*, 97(D14), 15 713-15 740.
- Ganopolski, A. et al., (2016)**, Critical insolation-CO₂ relation for diagnosing past and future glacial inception, *Nature*, 529, 200-203, doi: 10.1038/nature16494.
- Garner, A. J. et al., (2018)**, Evolution of 21st century sea level rise projections, *Earth's Future*, 6, 1603-1615, doi: 10.1029/2018EF000991.
- Gillet-Chaulet, F. et al., (2012)**, Greenland ice sheet contribution to sea-level rise from a new-generation ice-sheet model, *The Cryosphere*, 6, 1561–1576, doi: 10.5194/tc-6-1561-2012.
- Golledge, N. R. et al., (2019)**, Global environmental consequences of twenty-first-century ice-sheet melt, *Nature*, 566, 65-72, doi: 10/1038/s41586-019-0889-9.
- Haywood, A. M. et al., (2011)**, Pliocene Model Intercomparison Project (PlioMIP): Experimental Design and Boundary Conditions (Experiment 2), *Geoscientific Model Development* 4, 571-577, 2011, doi :10.5194/gmd-4-571-2011.
- Haywood, A. M. et al., (2016)**, The Pliocene Model Intercomparison Project (PlioMIP) Phase 2: scientific objectives and experimental design, *Climate of the Past*, 12, 663–675, doi:10.5194/cp-12-663-2016
- IMBIE team (2018)**, Mass balance of the Antarctic ice sheet from 1992-2017, *Nature*, 558, 219-222, doi: 10.1038/s41586-018-0179.

- IPCC (Ed.),** *Climate Change 2007: The Physical Science Basis; Contribution of Working Group I to the Fourth Assessment Report of the Intergovernmental Panel on Climate Change*, Cambridge, United Kingdom, and New-York, USA, Cambridge University Press.
- IPCC (Ed.),** *Climate Change (2013): The Physical Science Basis; Contribution of Working Group I to the Fifth Assessment Report of the Intergovernmental Panel on Climate Change*, Cambridge, United Kingdom, and New-York, USA, Cambridge University Press.
- Jevrejeva, S., Moore J. C., Grinsted, A., and. Woodworth, P. L., (2008),** Recent global sea level acceleration started over 200 years ago? *Geophysical Research Letters*, 35, L08715.
- Johnson, G. C. et al., (2007),** Recent bottom water warming in the Pacific Ocean, *Journal of Climate*, 20, 5365–5375.
- Keeling, C. D. et al., (1995),** Interannual Extremes in the Rate of Rise of Atmospheric Carbon Dioxide since 1980, *Nature*, 375, 666-670.
- Khodri, M. et al., (2001),** Simulating the Amplification of Orbital Forcing by Ocean Feedbacks in the Last Glaciation, *Nature*, 410, 570-574.
- Kopp, R. E. et al. (2009),** Probabilistic assessment of sea level during the last interglacial stage, *Nature*, 462, 863-867, doi: 10.1038/nature08686.
- Kouketsu, S., et al., (2011),** Deep ocean heat content changes estimated from observation and reanalysis product and their influence on sea level change. *Journal of Geophysical Research (Ocean)*, 116, C03012.
- Lambert, S. J. and Fyfe, J. C., (2006),** Changes in Winter Cyclone Frequencies and Strengths Simulated in Enhanced Greenhouse Warming Experiments: Results from the Models Participating in the IPCC Diagnostic Exercise, *Climate Dynamics*, 26, 713-728, doi: 10.1007/s00382-006-0110-3.
- Loutre, M.-F. and Berger, A., (2000),** Are We Entering an Exceptionally Long Interglacial?, *Climatic Change*, 46, 61-90.
- Luo, D., et al., (2016),** *Environmental Earth Science* 75: 555. doi: 10.1007/s12665-015-5229-2.
- Madden, R. A. and Julian, P. R., (1994),** Observations of the 40-50 Day Tropical Oscillation: a Review, *Monthly Weather Review*, 122, 814-837.
- Manabe, S. and Wetherald, R. T., (1967),** Thermal Equilibrium of the Atmosphere with a Given Distribution of Relative Humidity, *Journal of the Atmospheric Sciences*, 24 (3), 241-259, doi: 10.1175/1520-0469(1967)024<0241:TEOTAW>2.0.CO;2
- Meehl, G. A., Tebaldi, C., Walton, G., Easterling, D., and McDaniel, L., (2009),** Relative increase of record high maximum temperatures compared to record low minimum temperatures in the U.S. *Geophysical Research Letters*, 36, L23701, doi: 10.1029/2009GL040736.

- Nerem, R. S., Beckley, B. D., Fasullo, J. T., Hamlington, B. D., Masters, D., Mitchum G. T., (2018)**, Climate-change–driven accelerated sea-level rise, *Proceedings of the National Academy of Sciences*, 115 (9) 2022-2025; doi: 10.1073/pnas.1717312115
- Oerlemans, J., Van der Veen, C. J., (1984)**, *Ice Sheets and Climate*, Reidel, 217 pp.
- Oerlemans, J. (2005)**, Extracting a Climate Signal from 169 Glacier Records, *Science*, 308(5722), 675- 677.
- Peltier, D. F., et al. (2015)**, ICE-5G and ICE-6G models of postglacial relative sea-level history a Space geodesy constrains ice age terminal deglaciation: The global ICE-6G_C (VM5a) model, *Journal of Geophysical Research (Solid Earth)*, 120, 450–487.
- Purkey, S. G., and Johnson G. C., (2010)**, Warming of global abyssal and deep southern ocean waters between the 1990s and 2000s: Contributions to global heat and sea level rise budgets. *Journal of Climate*, 23, 6336–6351.
- Ramanathan, V. and Coakley, J. A. Jr., (1978)**, Climate Modeling Through Radiative-Convective Models, *Reviews of Geophysics and Space Physics*, 16(4), 465.
- Ramillien, G. et al. (2006)**, ‘Interannual Variations of the Mass Balance of the Antarctica and Greenland Ice Sheets from GRACE’, *Global and Planetary Change*, 53, 198-208.
- Ray, R. D., and Douglas, B. C., (2011)**, Experiments in reconstructing twentieth-century sea levels. *Progress in Oceanography*, 91, 495–515.
- Rignot E. et al. (2019)**, Four decades of Antarctic ice sheet mass balance from 1979-2017, *Proceedings of the National Academy of Sciences*, 116(4), 1095-1103, doi: 10.1073/pnas.18128883116.
- Rigor, I. G. and Wallace, J. M., (2004)**, Variations in the Age of Sea Ice and Summer Sea Ice Extent, *Geophysical Research Letters*, 31, doi: 10.1029 /2004GL019492.
- Romanovsky, V. E., S. L. Smith, and Christiansen, H. H., (2010a)**, Permafrost thermal state in the polar Northern Hemisphere during the International Polar Year 2007–2009: A Synthesis. *Permafrost Periglacial Processes*, 21, 106–116.
- Romanovsky, V. E. et al., (2010b)**, Thermal state of permafrost in Russia, *Permafrost Periglacial Processes*, 21, 136–155.
- Shepherd et al., (2012)**, A reconciled estimate of ice-sheet mass balance, *Science*, 338, 1183, doi: 10.1126/science.1228102
- Stott, P.A. et al., (2004)**, Human contribution to the European heatwave of 2003, *Nature*, 432, 610–614
- Szopa, S., et al., (2013)**, Aerosol and Ozone changes as forcing for Climate Evolution between 1850 and 2100, *Climate Dynamics*, 40(9-10), pp. 2223-2250, doi: 10.1007/s00382-012-1408-y.

- Tarasov, L, and Peltier, W. R., (2007)**, Coevolution of continental ice cover and permafrost extent over the last glacial-interglacial cycle in North America. *Journal of Geophysical Research*, vol. 112, F02S08, doi:10.1029/2006JF000661,
- Tschudi, M. A., Stroeve, J. C., & Stewart, J. S., (2016)**, Relating the age of Arctic sea ice to its thickness, as measured during NASA's ICESat and IceBridge campaigns. *Remote Sensing*, 8(6). <https://doi.org/10.3390/rs8060457>
- VandenBerghe, J., (2011), Permafrost during the Pleistocene in North West and Central Europe. Permafrost Response on Economic Development, Environmental Security and Natural Resources pp 185-194
- Vial, J. et al., (2013)**, On the interpretation of inter-model spread in CMIP5 climate sensitivity estimates; *Climate Dynamics*, 41(11-12), 3339-3362, doi: 10.1007/s00382-013-1725-9.
- Velicogna, I. and Wahr, J., (2006)**, Measurements of Time-Variable Gravity Show Mass Loss in Antarctica, *Science*, 311, 1 754-1 756.
- Velicogna, I. (2009)**, 'Increasing Rates of Ice Mass Loss from the Greenland and Antarctic Ice Sheets Revealed by GRACE', *Geophysical Research Letters*, 36 (L19503), doi: 10.1029/2009GLO4022.
- Velicogna, I. et al., (2014)**, Regional acceleration in ice mass loss from Greenland and Antarctica using GRACE time-variable gravity data, *Geophysical Research Letters*, 41, 8130–8137, doi: 10.1002/2014GL061052.
- WCRP Global Sea Level Budget Group (2018)**: Global sea-level budget 1993–present, *Earth Syst. Sci. Data*, 10, 1551-1590, <https://doi-org.insu.bib.cnrs.fr/10.5194/essd-10-1551-2018>.